

ESSA TR ERL 161-ITS 103

ESSA TR ERL 161-ITS 103

A UNITED STATES
DEPARTMENT OF
COMMERCE
PUBLICATION

ESSA Technical Report ERL 161-ITS 103

U.S. DEPARTMENT OF COMMERCE
Environmental Science Services Administration
Research Laboratories

An Analysis of the Shunt-Fed Log-Periodic Monopole Array Antenna

PITT WILLIS ARNOLD

BOULDER, COLO.
MARCH 1970



ESSA RESEARCH LABORATORIES

The mission of the Research Laboratories is to study the oceans, inland waters, the lower and upper atmosphere, the space environment, and the earth, in search of the understanding needed to provide more useful services in improving man's prospects for survival as influenced by the physical environment. Laboratories contributing to these studies are:

Earth Sciences Laboratories: Geomagnetism, seismology, geodesy, and related earth sciences; earthquake processes, internal structure and accurate figure of the Earth, and distribution of the Earth's mass.

Atlantic Oceanographic and Meteorological Laboratories and Pacific Oceanographic Laboratories: Oceanography, with emphasis on ocean basins and borders, and oceanic processes; sea-air interactions: and land-sea interactions. (Miami, Florida)

Atmospheric Physics and Chemistry Laboratory: Cloud physics and precipitation; chemical composition and nucleating substances in the lower atmosphere; and laboratory and field experiments toward developing feasible methods of weather modification.

Air Resources Laboratories: Diffusion, transport, and dissipation of atmospheric contaminants; development of methods for prediction and control of atmospheric pollution. (Silver Spring, Maryland)

Geophysical Fluid Dynamics Laboratory: Dynamics and physics of geophysical fluid systems; development of a theoretical basis, through mathematical modeling and computer simulation, for the behavior and properties of the atmosphere and the oceans. (Princeton, New Jersey)

National Severe Storms Laboratory: Tornadoes, squall lines, thunderstorms, and other severe local convective phenomena toward achieving improved methods of forecasting, detecting, and providing advance warnings. (Norman, Oklahoma)

Space Disturbances Laboratory: Nature, behavior, and mechanisms of space disturbances; development and use of techniques for continuous monitoring and early detection and reporting of important disturbances.

Aeronomy Laboratory: Theoretical, laboratory, rocket, and satellite studies of the physical and chemical processes controlling the ionosphere and exosphere of the earth and other planets.

Wave Propagation Laboratory: Development of new methods for remote sensing of the geophysical environment; special emphasis on propagation of sound waves, and electromagnetic waves at millimeter, infrared, and optical frequencies.

Institute for Telecommunication Sciences: Central federal agency for research and services in propagation of radio waves, radio properties of the earth and its atmosphere, nature of radio noise and interference, information transmission and antennas, and methods for the more effective use of the radio spectrum for telecommunications.

Research Flight Facility: Outfits and operates aircraft specially instrumented for research; and meets needs of ESSA and other groups for environmental measurements for aircraft. (Miami, Florida)

ENVIRONMENTAL SCIENCE SERVICES ADMINISTRATION

BOULDER, COLORADO 80302



U. S. DEPARTMENT OF COMMERCE

Maurice H. Stans, Secretary

ENVIRONMENTAL SCIENCE SERVICES ADMINISTRATION

Robert M. White, Administrator

RESEARCH LABORATORIES

Wilmot N. Hess, Director

ESSA TECHNICAL REPORT ERL 161-ITS 103

**An Analysis
of the Shunt-Fed Log-Periodic
Monopole Array Antenna**

PITT WILLIS ARNOLD

INSTITUTE FOR TELECOMMUNICATION SCIENCES
BOULDER, COLORADO
March 1970

For sale by the Superintendent of Documents, U. S. Government Printing Office, Washington, D. C. 20402
Price 65 cents



AN ANALYSIS OF THE SHUNT-FED LOG-PERIODIC
MONOPOLE ARRAY ANTENNA

by

Pitt Willis Arnold

B.S., University of Illinois, 1959

A thesis submitted to the Faculty of the Graduate
School of the University of Colorado in partial
fulfillment of the requirements for the degree of
Master of Science

Department of Electrical Engineering

1969

ABSTRACT

An analytic method is here introduced enabling one to insert the physical dimensions of a shunt-fed log-periodic monopole array antenna into a properly arranged computer program and obtain reasonably accurate information about the radiation and impedance characteristics of the antenna from the resultant computer output. The method is related to a similar analysis of dipole type antennas but the complexity of the feed system of the shunt-fed structures causes the matrix relations to be more complex than those of the dipole antenna. Computed and experimental results are compared and the "optimized feed" case is discussed at some length.

ACKNOWLEDGMENTS

The efforts of Lillie C. Walters, who programmed the matrix relations herein in the NBS-ESSA CDC 3800 computer, helpful discussions with Dr. Mark T. Ma, and the use of the experimental facilities at ESSA Research Laboratories are gratefully acknowledged.

TABLE OF CONTENTS

	<u>PAGE</u>
ABSTRACT	iv
ACKNOWLEDGMENTS	v
LIST OF TABLES	vii
LIST OF FIGURES	vii
SECTIONS	
I INTRODUCTION	1
II THE MATRIX RELATIONS	5
III THE COMPONENT MATRICES	9
A. The \bar{Z}_a Matrix and Relation Between Base-Fed and Shunt- Fed Monopoles	9
B. The \bar{Y}_s and \bar{Z}_c Matrices	19
C. The \bar{Y}_f Matrix	21
IV EXPERIMENTAL AND COMPUTED RESULTS	30
V CONCLUSIONS	38
BIBLIOGRAPHY	39
FIGURES	42

LIST OF TABLES

		<u>PAGE</u>
1	Y'_{O_n} and V'_{P_n} Calculations for Case A_3	27

LIST OF FIGURES

1	Photograph of a Wire-Outline Shunt-Fed Log-Periodic Monopole Array	42
2	Photograph of a Shunt-Fed Log-Periodic Monopole Array with Cylindrical Monopoles	43
3	Geometry of Log-Periodic Monopole Arrays Showing Two Adjacent Monopoles	44
4	Diagram of a Two-Element Shunt-Fed Array Illustrating Equivalent Circuit Elements and Node Current Relations	45
5	Geometry and Notation Used in Mutual Impedance Calculations	46
6	Resonant Impedance of a Shunt-Fed Monopole as a Function of Feedpoint Height with Height to Radius Ratio as Parameter	47
7	Current Distribution on a Shunt-Fed Monopole vs. Probe Height with Feed-Point Height as a Parameter	48
8	Current Distribution on a Grounded Monopole vs. Probe Height. Current Induced by Adjacent Shunt-Fed Monopole of Equal Height. Feed-Point Height is Parameter .	49

9	Input Impedance vs. Frequency of a Shunt-Fed Monopole and a Base-Fed Monopole with a Matching Network	50
10	Locus for Z_O and V_p Determination for Case A_3	51
11	Locus for Z_O and V_p Determination for Case C_3	52
12	Measured and Calculated Radiation Patterns for Case C_3 in Azimuth Plane	53
13	Measured and Calculated Radiation Patterns for Case D in Azimuth Plane	54
14	Input Impedance of Wire-Outline Monopole Array vs. Frequency for Case A_3	55
15	Input Impedance of Wire-Outline Monopole Array vs. Frequency for Case C_3	56
15A	A Comparison of Calculated Impedances for Case C_3	57
16	Average Characteristic Impedance and VSWR of Cases A and B. A Comparison of Measured and Calculated Data	58
17	Input Impedance of Cylindrical Monopole Array vs. Frequency for Case D	59
18	Computed Self Impedances for Monopoles as a Function of Electrical Length, in Radians, for Constant h/a	60

INTRODUCTION

The shunt-fed log-periodic monopile array antenna, two types of which are shown in Figures 1 and 2, is an array of grounded monopoles whose heights, spacings, and effective diameters increase from the front or feed end of the structure by a fixed proportionality constant. Properly functioning antennas of this type exhibit essentially frequency independent radiation patterns and impedance loci within their operating frequency range. Their usable frequency range has a lower limit defined approximately by the frequency where the rear, or tallest, monopole is one-quarter wavelength in height and an upper limit defined by the frequency where the shortest element is three-sixteenths of a wavelength in height. Their radiation patterns are usually single lobed, with the maximum radiation along the line of the monopoles in the direction of the smaller elements. The phasing required for this direction of radiation is produced by a combination of factors, the net result being an effective reduction in phase velocity, in the feed system, between the monopoles near their resonant frequencies. The beamwidth of the radiation pattern depends on the number of radiating monopoles and on the choice of log-periodic parameters.

Wickersham's^{1,2} "Ladder" antenna was one of the first shunt-fed log-periodic monopole arrays built. It used metal blades as monopoles which were trapezoidal in shape like the monopoles of the Wire-Outline antenna developed by Ore,³ and shown in Figure 1. These two types are quite similar. The antenna pictured in Figure 2 was developed by the author for a high-power HF radar application where 10 of these antennas are arrayed together. It is a one-hundredth scale model and operates between 700 and 2500 MHz to simulate the 7-25 MHz full-scale antenna. The shunt-fed type of monopole array with cylindrical monopoles appears well suited for this application. All three types of shunt-fed arrays mentioned above use metal cylinders, which are fastened to the monopoles at a fixed percentage of a monopole's total height and are coaxial to the feed rod, thus forming a coupling capacitor. The feed rod is connected to the center conductor of a coaxial feedline at a point just in front of the first monopole and its capacitor. The outer conductor of this coaxial line is connected to the ground plane near the same point. Most of the models built have had this coaxial line come in beneath and perpendicular to the metal ground plane, although it might be arranged to come in perpendicular to the feed rod and parallel to and contacting the

ground plane. The geometry of the array is given in Figure 3 showing two monopoles of an array. The envelope of the element tips makes an angle α with the ground plane and intersects it at the virtual vertex. The constant τ relates the heights, spacings and widths, or effective diameters, of adjacent monopoles; τ and α are related to σ , the spacing constant, by $\sigma = \frac{1}{2}(1-\tau) \cot \alpha$. These constants are those commonly used to describe log periodic dipole arrays as in the work of Isbell⁴ and in the analysis of Carrel.⁵

With the exception of an investigation by Hudock and Mayes⁶ into the near-field properties of uniformly-periodic monopole arrays, little, if any, analytical work has been published on these antennas. No attempts to relate their behavior to the log-periodic dipole arrays have been made nor has any analysis been made of them in terms of network theory. This lack of definitive analyses together with some unusual experimental results, obtained during the earlier development of the antenna in Figure 2 prompted this analysis. The unusual experimental results showed that a feed network parameter; specifically the capacitor lengths y_n , should be varied in other than log-periodic fashion to obtain the best or "optimum" input impedance vs. frequency. These results were obtained without prior knowledge of Ore's similar findings.⁷

The method herein, of necessity, follows the lead of Carrel,⁸ who first analyzed the transposed feeder log-periodic dipole array using circuit theory and matrix algebra. The antenna impedance matrix is derived as Carrel derived it, but an additional two-element passive network is connected between the monopoles and the transmission line. This two-element network causes the base-fed monopoles used in the computer program to appear as an approximation to shunt-fed monopoles, both with respect to input impedance and current phase shift as viewed from the coupling capacitor connection points, or nodes.

The matrix algebra is presented first, showing the relations between the matrices to be individually described later. The manner of calculation of the antenna impedance matrix and the relation between base-fed and shunt-fed monopoles are then discussed. The method for calculating the elements of the network and related matrices is then described, followed by a description of feeder admittance matrix calculation. Finally, the computed and measured radiation patterns and impedance loci, for the antennas in Figures 1 and 2 are presented and discussed. The impedance "optimization" method is also discussed.

II

THE MATRIX RELATIONS

The circuit shown in Figure 4 represents two shunt-fed monopoles and their associated transmission line. Application of elementary circuit theory permits extension of the following to N monopole elements.

The passive elements connected between the unprimed nodes and the primed nodes, as well as the passive elements connected between the unprimed nodes and the ground are assumed to have no interconnection other than that shown and thus can be represented in the matrix relations by a simple 2, or N, element diagonal matrix. The elements shown as resistors represent 2, or N, intercoupled base-fed, gapless monopoles and thus are represented by a 2X2, or NXN, matrix. The transmission line is represented by an admittance matrix having only diagonal and sub-diagonal entries, since there are only direct connections between a node and its immediate neighbors. Matrix quantities are indicated by a bar above the voltage, current, impedance, or admittance symbol.

At the unprimed nodes, a summation of currents gives

$$\bar{I}'_a = \bar{I}_a + \bar{I}_s \quad , \quad (1)$$

or, in matrix notation,

$$\bar{I}'_a = \bar{I}_a + \bar{I}_s \quad (2)$$

or

$$\bar{I}'_a = \bar{Y}_a \bar{V}_a + \bar{Y}_s \bar{V}_s \quad (3)$$

Since \bar{V}_a and \bar{V}_s are the same, (3) may be written as

$$\bar{I}'_a = (\bar{Y}_a + \bar{Y}_s) \bar{V}_a \quad (4)$$

Since we wish to introduce the element impedance matrix and solve for the element currents, we introduce the relation

$$\bar{V}_a = \bar{Z}_a \bar{I}_a \quad (5)$$

into (4) to obtain

$$\bar{I}'_a = (\bar{Y}_a + \bar{Y}_s) \bar{Z}_a \bar{I}_a = (\bar{U} + \bar{Y}_s \bar{Z}_a) \bar{I}_a \quad (6)$$

where \bar{U} is the unit matrix.

Moving now to the primed nodes and again summing currents we obtain

$$I_{in} = I_f + I'_a \quad (7)$$

or, using matrix notation,

$$\bar{I}_{in} = \bar{I}_f + \bar{I}'_a \quad . \quad (8)$$

Since

$$\bar{I}_f = \bar{Y}_f \bar{V}_f \quad , \quad (9)$$

and

$$\bar{V}_f = \bar{V}_c + \bar{V}_a = \bar{Z}_c \bar{I}'_a + \bar{Z}_a \bar{I}_a \quad , \quad (10)$$

(7) becomes

$$\bar{I}_{in} = \bar{Y}_f [\bar{Z}_c \bar{I}'_a + \bar{Z}_a \bar{I}_a] + \bar{I}'_a = [\bar{U} + \bar{Y}_f \bar{Z}_c] \bar{I}'_a + \bar{Z}_a \bar{I}_a \quad . \quad (11)$$

Substituting the relation for \bar{I}'_a , or (6), into (11), we obtain

$$\bar{I}_{in} = \{[\bar{U} + \bar{Y}_f \bar{Z}_c][\bar{U} + \bar{Y}_s \bar{Z}_a] + \bar{Z}_a\} \bar{I}_a \quad . \quad (12)$$

The column matrix \bar{I}_{in} has only one non-zero element, the input current to the antenna array, which we conveniently assign a unit value. All the quantities in the large brackets of (12) may be calculated or are known. Therefore, we may solve for \bar{I}_a , the column matrix of element currents, by matrix inversion. Let the bracketed quantities of (12) be called \bar{X} . Then (12) becomes

$$\bar{I}_{in} = \bar{X} \bar{I}_a \quad . \quad (13)$$

Pre-multiplying each side by \bar{X}^{-1} gives

$$\bar{I}_a = \bar{X}^{-1} \bar{I}_{in} . \quad (14)$$

Since the values of \bar{I}_a are now known, we may solve for the input voltage, which will give us the input impedance, since the input current is assumed to be one ampere. The relation used is

$$\bar{V}_f = \{ \bar{Z}_c [\bar{U} + \bar{Y}_s \bar{Z}_a] + \bar{Z}_a \} \bar{I}_a , \quad (15)$$

from which we take V_{f_1} to obtain the impedance. Equation (14) is programmed in a computer to obtain element currents, from which radiation patterns may be obtained with an additional computation. The input impedance of the antenna is then obtained from (15). The \bar{Z}_a , \bar{Y}_s , \bar{Z}_c , and \bar{Y}_f matrices must first be calculated, preferably with the computer, and the methods of calculating them are treated next.

III

THE COMPONENT MATRICES

A. The \bar{Z}_a Matrix and Relation Between Base-Fed and Shunt-Fed Monopoles.

The description to follow closely parallels that of Carrel⁹ and uses the method of induced-emf as applied to unequal length dipoles by H. E. King.¹⁰ The following assumptions and/or approximations are made:

- (1) A symmetric sinusoidal current distribution is assumed over the dipole formed by a monopole and its image in the ground plane. This is reasonably valid where a monopole is less than one-half wavelength long, the accuracy being greatest for quarter wave and shorter monopoles. Accuracy is improved by avoiding frequencies where any monopole is within a few percent of one-half wavelength. Greater accuracy can be obtained, by following Cheong¹¹ and Cheong and King^{12,13} with three-term formulation of the currents.
- (2) In the calculation of mutual impedances, the elements are assumed to be infinitesimally

thin; i.e., the current at a cross-section of the actual dipole has been replaced by an average current concentrated at the center of the cross section.

- (3) The mutual term involves only the two elements considered; i.e., the intervening elements are neglected. This assumption is actually implicit in (2) above. In the limiting case of zero element thickness, the current in the first dipole induces a voltage across the terminals of the second but no current along it, since the inductance per unit length of an infinitesimally thin dipole is infinite. Since there is no induced current, there is no voltage across any other dipole from the induced current in the second dipole, and therefore no secondary action.
- (4) The self-impedances are calculated from the same formula as the mutuals by approximating the self-impedance of a dipole of radius a as the mutual impedance of two infinitesimally thin dipoles spaced a distance $\sqrt{2}a$ apart.¹⁴

Figure 5 shows two parallel symmetrical dipoles, of half-lengths h_1 and h_2 , separated by distance s ,

with element dz at coordinate distance z from the x - y plane. The distances r_0 , r_1 , and r_2 are distances from fixed points on one dipole to a typical element on the other. The mutual impedance between the two antennas in Figure 5 may be defined by

$$Z_{21} = \frac{-V_{21}}{I_1(0)} \quad , \quad (16)$$

where V_{21} is the open circuit voltage at the terminals of antenna 2 caused by a center current $I_1(0)$ at the terminals of antenna 1. The voltage V_{21} is given by^{15,16}

$$V_{21} = \frac{1}{I_2(0)} \int_{-h_2}^{h_2} E_{z_1} I_2(z) dz \quad , \quad (17)$$

where E_{z_1} is the z component of electric field intensity at the location of antenna 2 caused by the current of antenna 1, when antenna 2 is removed. The current distribution on antenna 2 is assumed to be sinusoidal and is given by

$$I_2(z) = I_{2\max} \sin \beta(h_2 - |z|) \quad , \quad (18)$$

where β is the free-space propagation constant. The expression for the z component of electric field caused by a sinusoidally distributed current in antenna 1 is given by

$$E_{z_1} = -j30I_{1\max} \left[\frac{e^{-j\beta r_1}}{r_1} + \frac{e^{-j\beta r_2}}{r_2} - \frac{2 \cos \beta h_1 e^{-j\beta r_0}}{r_0} \right] . \quad (19)$$

Inserting (18) and (19) into (16) and (17) gives the mutual impedance referred to the base of the antenna,

$$Z_{12} = Z_{21} = j30 \frac{I_{1\max} I_{2\max}}{I_1(0) I_2(0)} \int_{-h_2}^{h_2} \sin \beta(h_2 - |z|) \left[\frac{e^{-j\beta r_1}}{r_1} + \frac{e^{-j\beta r_2}}{r_2} - \frac{2 \cos \beta h_1 e^{-j\beta r_0}}{r_0} \right] dz \quad (20)$$

and with the assumption of sinusoidal currents the maximum currents are related to the base currents by

$$I_1(0) = I_{1\max} \sin \beta h_1 , \quad (21)$$

$$I_2(0) = I_{2\max} \sin \beta h_2 ,$$

and from Figure 5

$$r_0 = \sqrt{s^2 + z^2} ,$$

$$r_1 = \sqrt{s^2 + (h_1 - z)^2} , \quad (22)$$

$$r_2 = \sqrt{s^2 + (h_1 + z)^2} .$$

Therefore, (20) may be rewritten as

$$Z_{12} = j30 \csc \beta h_1 \csc \beta h_2 \int_{-h_2}^{h_2} \sin \beta (h_2 - |z|) \left[\frac{e^{-j\beta r_1}}{r_1} + \frac{e^{-j\beta r_2}}{r_2} - \frac{2 \cos \beta h_1 e^{-j\beta r_0}}{r_0} \right] dz \quad (23)$$

Integration of (23) gives an expression for the mutual impedance in terms of sine and cosine integral functions.

$$Z_{12} = \frac{60}{\cos w_2 - \cos w_1} \left\{ e^{jw_1} [K(u_0) - K(u_1) - K(u_2)] + e^{-jw_1} [K(v_0) - K(v_1) - K(v_2)] + e^{jw_2} [K(u'_0) - K(u_1) - K(v_2)] + e^{-jw_2} [K(v'_0) - K(v_1) - K(u_2)] + 2K(w_0) [\cos w_1 + \cos w_2] \right\}^* \quad (24)$$

where * denotes the complex conjugate of the expression in the braces and

$$K(x) = Ci(x) + jSi(x)$$

$$= \int_{\infty}^x \frac{\cos y}{y} dy + j \int_0^x \frac{\sin y}{y} dy \quad (25)$$

The other quantities in (24) are defined below.

$$\begin{aligned}
u_0 &= \beta \left[\sqrt{s^2 + (h_1 + h_2)^2} - (h_1 + h_2) \right] , \\
v_0 &= \beta \left[\sqrt{s^2 + (h_1 + h_2)^2} + (h_1 + h_2) \right] , \\
u'_0 &= \beta \left[\sqrt{s^2 + (h_1 - h_2)^2} - (h_1 - h_2) \right] , \\
v'_0 &= \beta \left[\sqrt{s^2 + (h_1 - h_2)^2} + (h_1 - h_2) \right] , \\
u_1 &= \beta \left[\sqrt{s^2 + h_1^2} - h_1 \right] , \\
v_1 &= \beta \left[\sqrt{s^2 + h_1^2} + h_1 \right] , \\
u_2 &= \beta \left[\sqrt{s^2 + h_2^2} - h_2 \right] , \\
v_2 &= \beta \left[\sqrt{s^2 + h_2^2} + h_2 \right] , \\
w_1 &= \beta (h_1 + h_2) , \\
w_2 &= \beta (h_1 - h_2) , \\
w_0 &= \beta s .
\end{aligned} \tag{26}$$

The mutual and self-impedances of a log-periodic monopole array may then be calculated by suitably programming the lengths, spacings and length to radius ratio in a digital computer. The formulation presented above yields the self and mutual impedances of an array

of dipoles. Dividing all values obtained by 2 gives the \bar{Z}_a matrix for a monopole array.

The \bar{Z}_a matrix obtained is for base-fed monopoles having no gap at the feedpoint. How can we relate the base-fed monopole to the actual monopole used, one which is grounded and fed at some distance above the base? At first, the method of impedance calculation suggested by Morrison and Smith¹⁷ was tried, wherein the portion of the antenna between the feedpoint and the ground is assumed to be a shunt inductor and the portion above the feedpoint is assumed to be a base-fed structure of height equivalent to the height above the feedpoint. This proved to be less than satisfactory because of the difficulty of calculating the inductive reactance of the portion of antenna below the feedpoint. It was decided instead to measure the actual impedance vs. frequency of shunt-fed monopoles for several different feedpoint heights and monopole diameters, and use a network that would best approximate the impedance of a shunt-fed monopole when used with the base-fed monopole. Figure 6 gives the resonant impedance of shunt-fed monopoles of three different height to radius ratios as a function of feedpoint height H/h . This information allows the design of a network which will match the approximately

34 ohm resonant impedance of a base-fed monopole to the resonant impedance of a shunt-fed monopole of specified feedpoint height. This is not enough, since we must also simulate the phase shift between the input current to the shunt-fed monopole and the radiation current. Also we must approximate the impedance vs. frequency characteristics of the shunt-fed monopole. The desired phase shift information was obtained from Figures 7 and 8 by the following reasoning.

For continuity of current at the feedpoint of an isolated shunt-fed monopole we may assume that the input current I_{in} is equal to $I_s + I_a$, where I_s is the current flowing toward the earth in the monopole shown in Figure 6 and I_a is flowing upward from the feedpoint. With these assumed current directions, a sensing probe near the antenna will sample $I_s - I_a$ or $I_a - I_s$. Call this difference I_m . Figure 7 shows this measured difference current as a function of probe height z for two different feedpoint heights. Figure 8, which shows the measured current of a parasitically excited monopole of the same height and radius as the monopole in Figure 7 is of the assumed sinusoidal form of the base-fed monopoles of our \bar{Z}_a formulation. The radiation current of the shunt-fed monopole, or I_a , is assumed to be of this form also. Referring again to Figure 7, for

the case of $H/h=0.126$ and taking the readings for $z=11\text{cm}$, we note that there is little phase change above $z=11\text{cm}$ and that the magnitude of I_m seems to be varying as in Figure 8. We then assume that we are measuring I_a only at $z=11\text{cm}$ and according to Figure 8 I_a has reached one-half its maximum at $z=11\text{cm}$. We therefore conclude that near the base, or even at the feedpoint, the I_a of the antenna in Figure 7 is $0.7e^{-j56^\circ}$. The measured feedpoint current $I_{in}=I_a-I_s$ is $0.69e^{-j18^\circ}$. We wish to know I_{in} in terms of I_a in order to establish at least the direction of phase shift which our equivalent circuit should introduce. Adding the two relations $I_m=I_a-I_s$ and $I_{in}=I_a+I_s$, we obtain $I_{in}=2I_a-I_m$. Substituting the values deduced above, we obtain $I_{in}=0.96e^{-j82^\circ}$ which lags I_a by 26° . A similar treatment of the $H/h=0.088$ case shows I_{in} lagging I_a by 30° . The required circuit is seen to be one which will introduce a phase lag between I_a and I_{in} which is dependent on feedpoint height H , and therefore dependent on the required transformation ratio between a base-fed monopole's resonant impedance of about 34 ohms and that of a shunt-fed monopole of feedpoint height H . A two-element network which has about the correct phase shift characteristics and whose impedance vs. frequency characteristic, when matching a base-fed monopole to a lower impedance, is a fair approximation to the impedance of a shunt-fed monopole

is a shunt inductance series capacitance L network. For practical feedpoint heights and monopole height to radius ratios, a reduction to a value between 8 and 12 ohms is usually called for, as experimental data will later show. Therefore, this form of matching network will suffice in most cases.

The degree of approximation to the impedance vs. frequency characteristic of a shunt-fed monopole, with $h/a=14$ and $H/h=0.126$, obtained with an L network is shown in Figure 9. Better agreement is obtained below f_0 , the resonant frequency, than above f_0 . This is perhaps fortunate since the monopoles or dipoles in front of the resonant one are usually more of a factor in log-periodic monopole and dipole structures than are those behind it. It should be stressed at this point that the shunt inductor and series capacitor of the L network are not intended to simulate the reactance below the feedpoint as in the much earlier work of Morrison and Smith,¹⁸ but, instead, are intended to make the base-fed monopole, whose impedance is easily computer simulated, approximately equivalent to the shunt-fed monopole. Resonance in a shunt-fed monopole occurs at about the same electrical length as it does in the base-fed monopole, but the locus (see Figure 9) has the form of an anti-resonant circuit. The measured locus in

Figure 9 might be more closely duplicated analytically by considering it as a lossy, tapped transmission line having varying characteristic impedance and attenuation along its length, but such an analysis would little suit our purpose here due to its complexity.

B. The \bar{Y}_S and \bar{Z}_C Matrices.

The \bar{Y}_S matrix is seen to be a diagonal matrix consisting of the shunt inductors of L networks, which match the resonant impedance of a base-fed monopole of known h/a ratio to the resonant impedance of a shunt-fed monopole of the same h/a and known H/h. Any single monopole may be calculated first at its resonant frequency and the rest are then calculated by using the scaling constant τ . For example, the monopole in Figure 9 has a resonant impedance, in the shunt-fed configuration, of 9 ohms. This resonance occurs at a frequency where $h \approx 0.226\lambda$. The base-fed monopole having the same h/a also resonates where $h \approx 0.226\lambda$ and has an impedance of 33.5 ohms. With these two values known we may compute Y_S from

$$Y_S = \frac{1}{jR_2} \sqrt{\frac{R_2 - R_1}{R_1}} \quad (27)$$

With $R_2=33.5$ and $R_1=9$, a value of $-j.049$ mhos is obtained.

The remainder of the Y_s values are then easily calculated from

$$Y_{s_n} = \tau Y_{s_{n-1}} \quad . \quad (28)$$

The \bar{Z}_c matrix is also a diagonal matrix of imaginary terms, but it consists of two parts, one of which is the required L network series capacitor. This may be calculated for a resonant monopole from

$$-jX_{c_e} = -j\sqrt{(R_2 - R_1)R_1} \quad , \quad (29)$$

where R_2 and R_1 are the resonant impedances of the base- and shunt-fed monopoles respectively. For Figure 9, $-jX_{c_e} = -j14.9$ ohms. The rest of the values may be obtained from

$$Z_{c_{e_n}} = \tau Z_{c_{e_{(n+1)}}} \quad . \quad (30)$$

The other part of the \bar{Z}_c matrix is the physical coupling capacitor, C_{c_n} , which is in series with C_{e_n} and is calculated from

$$Z_{c_{c_n}} = -jZ_{c_o} \cot \beta y_n \quad , \quad (31)$$

where y_n is the physical length of the air dielectric coupling capacitor, and Z_{c_0} is the characteristic impedance of the coaxial capacitor.

C. The \bar{Y}_f Matrix.

A brief discussion of the three regions of a log-periodic structure may be helpful before describing the method of calculation of the \bar{Y}_f matrix values. Carrel¹⁹ calls these three regions the transmission region, the active region, and the unexcited region.

The front or transmission region contains monopoles which are shorter than their resonant lengths, thus they absorb little energy from the line and in conjunction with their feed capacitors serve only to load the feedline and reduce its impedance and velocity of propagation. The energy entering the active region encounters monopoles which load the line with resistive impedances, thus absorbing energy and radiating it into space. The remaining energy enters the unexcited region and since this region contains mostly reactive impedances, the energy is reflected back into the active region. The amount of energy entering the unexcited region is usually quite small in a successful design. The upper frequency limit of a log-periodic structure is reached

when there is no longer a transmission region on the antenna, and the lower frequency limit is reached when there is no longer an unexcited region on the antenna.

For calculating the \bar{Y}_f matrix components, I assume that the entire antenna is being operated in the transmission region and that the components of the \bar{Z}_c matrix, which we assume in our matrix formulation are lumped at the monopole feedpoints, can be assumed as distributed along the feed rod. In fact, we assume that the entire antenna is a tapered transmission line with uniform impedance between monopoles, whose inductance per unit length and capacity per unit length may be obtained, for each section, from

$$L'_n = \frac{Z_{o_n}}{V_p} \quad (32)$$

and

$$C'_n = \frac{1}{Z_{o_n} V_p} \quad (33)$$

where the nth section is between monopoles n and n+1, Z_{o_n} is the characteristic impedance of a section, and V_p is the velocity of propagation of all sections. Before proceeding with the calculation of the \bar{Y}_f matrix, we must obtain the V_p and Z_{o_n} quantities. This was

first done experimentally for all the cases later treated mathematically and experimentally. These measurements of V_p and Z_o are shown, for two cases, in Figures 10 and 11. (V_p and Z_o may also be calculated using formulas developed from the V_p and Z_o measurements, which will be given later.) Figure 10 will be used for the following explanation of V_p and Z_o calculation. It shows a circular locus of impedances on a Smith chart whose nominal impedance is 50 ohms. (All Smith charts in this thesis will have a nominal impedance of 50 ohms unless otherwise specified.) This locus is for a monopole array having 6 monopoles and 5 sections of transmission line, each with a different impedance. The higher measured resistive impedance, or R_2 , has a value of about 125 ohms, and the lower value, or R_1 , is about 49 ohms. We may then assume that the average Z_o of the equivalent line is

$$Z_{o_{avg}} = \sqrt{R_2 R_1} = 78.2 \text{ ohms} \quad . \quad (34)$$

At the higher resistive impedance point, we assume that the line is one-half wavelength long and accordingly transforms the 150 ohm load impedance by the ratio Z_{o_5}/Z_{o_1} . Then we have

$$Z_{O_5}/Z_{O_1} = R_L/R_2 = 1.2 \quad (35)$$

and

$$\sqrt{Z_{O_5} Z_{O_1}} = Z_{O_{avg}} = 78.2 \text{ ohms} \quad (36)$$

Solving (35) and (36) we obtain Z_{O_1} and Z_{O_5} values of 71.5 ohms and 85.8 ohms, respectively. We then calculate the other sections' impedances from

$$Z_{O_n} = Z_{O_1} (1.2)^{\frac{n-1}{4}} \quad (37)$$

The V_p may also be calculated from the locus of Figure 10 provided certain precautions are taken. It has been found that the most reliable V_p values are obtained by using the lower frequency resistive crossover, about 120 MHz in Figure 10, and by assuming that this is the frequency where the line is an electrical quarter wave. The frequency where this line is a physical quarter wavelength is 188 MHz. Taking the ratio of the electrical to physical quarter wavelength frequencies and multiplying by 3×10^8 gives a V_p of 1.92×10^8 m/sec. If the higher frequency resistive crossover is used, and is assumed to be the electrical half-wavelength frequency, a lower V_p is obtained, which is not consistent with the

low frequency approximation being made, since the coupling capacitors no longer have capacity values directly proportional to their physical lengths.

We now have the Z_{o_n} values and V_p , which we assume is constant for all sections. We must then remove the shunting effect of the series combination of capacitors making up the \bar{Z}_c matrix. This is done, however, for a very low frequency where the coupling capacitor will have a value of

$$C_{c_n} = \frac{10^4}{3Z_{c_o}} y_n \text{ picofarads} , \quad (38)$$

where y_n is the length of a capacitor in meters. (We also assume that the Y_s and Z_a values are infinite at these frequencies.)

The series capacitor of the L network may be calculated from

$$C_{e_n} = \frac{1}{\omega_o X_n} \text{ farads} , \quad (39)$$

where X_n is the calculated reactance value at f_o and $\omega_o = 2\pi f_o$. One-half of the series combination of the above two capacitors plus one-half the series combination of the (n+1)th monopole's capacitors is assumed to

be distributed along the nth section of line. This combination, converted to a per unit length capacity, must then be subtracted from C_n' to yield a new quantity C_n'' , which will be used with the calculated value of L_n' to obtain new values of Z_{O_n}' and V_{P_n}' for the \bar{Y}_f matrix. The diagonal or self-admittance terms will be

$$Y_{f_{nn}} = -jY_{O_n}' \cot \beta's_n - jY_{O_{n-1}}' \cot \beta's_{n-1}, \quad (40)$$

and the off diagonal terms will be

$$Y_{f_{n,n+1}} = jY_{O_n}' \csc \beta's_n, \quad (41)$$

where

$$\beta's_n = \left(\frac{3 \times 10^8}{V_{P_n}'} \right) \beta s_n. \quad (42)$$

Here s_n is the space between the centers of the nth and (n+1)th monopoles and β is $2\pi/\lambda$. A tabulated calculation for the case treated in Figure 10 is given in Table 1. The last line of this table is the half-section between the first node, where the input impedance is calculated, and the actual input terminal of the antenna. The true input impedance is obtained from

Table 1. Y'_{O_n} and V'_{P_n} CALCULATIONS FOR CASE A₃

n	Z_{O_n} (ohms)	$\frac{Z'_{O_n}}{L_n V_p}$ (H/m)	$C'_n = \frac{1}{Z'_n V_p}$ (pF/m)	C_{e_n} (pF)	C_{c_n} (pF)	$C_{T_n} = \frac{C_{e_n} C_{c_n}}{C_{e_n} + C_{c_n}}$ (pF)	S_n (cm)	$C'_{T_n} = \frac{C_{T_n} + C_{T_n}}{2S_n}$ (pF/m)	$C_n = C_n - C_{T_n}$ (pF/m)	$Z'_{O_n} = \sqrt{\frac{L'_n}{C'_n}}$ (ohms)	$\frac{Z'_{O_n}}{V'_n L_n}$ (m/sec)	$\frac{3 \times 10^8}{V'_n P_n}$	Y'_{O_n} (mhos)
1	71.5	37.2×10^{-8}	72.7	4.69	1.41	1.08	2.75	47.6	25.1	121.5	3.26×10^8	0.92	0.0082
2	74.8	39.0×10^{-8}	69.5	6.78	1.99	1.54	3.88	48.1	21.4	135.0	3.47×10^8	0.866	0.0074
3	78.4	40.8×10^{-8}	66.5	9.58	2.85	2.19	5.5	48.2	18.3	149.0	3.65×10^8	0.823	0.0067
4	82.0	42.7×10^{-8}	63.5	13.55	4.06	3.12	7.76	48.7	14.8	170.0	3.98×10^8	0.755	0.0059
5	85.8	44.6×10^{-8}	60.6	19.16	5.76	4.43	11.0	48.5	12.1	192.0	4.3×10^8	0.700	0.0052
6				27.1	8.12	6.25							
0	71.5	37.2×10^{-8}	72.7				1.4	36.0	36.7	100.5	2.69×10^8	1.11	

$$Z'_{in} = Z'_{o_o} \left[\frac{Z_{in} + jZ'_{o_o} \tan \beta's_o}{Z'_{o_o} + jZ_{in} \tan \beta's_o} \right] \quad (43)$$

where Z'_{o_o} is the characteristic impedance of the input half-section, Z_{in} is the computed value of V_{f_1} from equation (15), and $\beta's_o$ is the electrical distance between the input connector and node no. 1'.

Two formulas for calculating Z_{o_n} and V_p have been developed from the V_p and Z_o measurements. They work well with the two antennas shown in Figures 1 and 2, but their validity for values of τ greater than .82 and less than .707 has not been checked. They are

$$Z_{o_n} = \frac{.565}{\tau} \left[\sqrt{Z_{L_n} Z_{c_o}} \right] \frac{\tau'}{\tau}^{\frac{n-1}{3}} \quad (44)$$

and

$$V_p = \frac{2.66 \times 10^8 \tau'}{\tau^2} \sqrt{\frac{Z_{c_o}}{Z_{L_n \text{ avg}}}} \quad (45)$$

where Z_{L_n} is the average impedance of the feed rod with respect to the ground plane for section n if we assume it is in the clear; Z_{c_o} is the characteristic impedance of

the feed capacitors; $Z_{L_{n_{avg}}}$ is the geometric mean of Z_{L_1} and Z_{L_N} ; τ is the log-periodic scaling constant and τ' is the scaling constant for the capacitor lengths, which may be greater than or equal to τ .

IV

EXPERIMENTAL AND COMPUTED RESULTS

Four cases were measured and computed. Three of these cases, Cases A, B and C, used the monopole array of Figure 1 with different feedline configurations. Two of the cases, Cases A and B, had sub-cases A2, A3, A4 and B2, B3, B4. The number following the letter indicates the angle of the feed rod with respect to the ground plane. These feed rod angles correspond to feedpoint heights of $H/h=0.0845$, 0.126 and 0.169 , respectively. Cases A and B have a good impedance match, for the height of feed producing the best match, over only a portion of the design frequency range and are not considered usable antennas. They were investigated mostly for comparison with the data given by Ore,²⁰ which proved difficult since it is not known for what portion of the frequency range he quotes average characteristic impedance and VSWR. For comparison with my computed data, the octave of frequency from 720 to 1440 MHz was used, as this is about the center of the theoretical design bandwidth of 500 to 1800 MHz. The model used for Cases A, B, and C has a τ of 0.707, an α angle of 22.5° , and the height to radius ratio of the wire

outline monopoles is 14, with the equivalent radius a_n calculated from

$$a_n = \sqrt{R_n W_n} \quad , \quad (46)$$

where R_n is the average radius of the two uprights, and W_n is their center to center spacing.²¹

Case A has a Z_{c_0} of 52 ohms and the τ' scaling constant for the capacitor lengths is equal to τ . The capacitors occupy almost the full space allotted them, or y_n is almost $\tau^{\frac{1}{2}}$ times s_n . Sub-cases 1, 2 and 3 differ only in the point of attachment of the capacitors.

Case B is the same as A except that Z_{c_0} is 73 ohms.

Case C is an "optimized" feed case, where Z_{c_0} and τ' have been adjusted to obtain a good impedance match to a 50 ohm line over the entire frequency band; Z_{c_0} is 42.8 ohms and τ' is 0.8.

Case D is the antenna in Figure 2 which has 11 cylindrical elements of $h/a=60$, a τ of 0.82, an α angle of 16.7° , a feedpoint height $H_n = 0.1h_n$, a Z_{c_0} of 33.5 ohms, and a τ' of 0.88. It is also an "optimized" design.

Figure 12 is a comparison of calculated and measured radiation patterns for Case C or C_3 . This is a

typical pattern for the entire usable frequency range of this antenna. The calculated pattern was obtained using the element currents calculated from equations (12) and (14) in the expression

$$E_{\theta}(\phi, \frac{\pi}{2}) = K \sum_{n=1}^N I_n e^{-j\beta(X_n \cos \phi) x(1-\cos \beta h_n)}, (47)$$

where I_n is the element current, a complex number; X_n is the element distance from the virtual vertex, measured along the array; ϕ is the azimuthal angle with respect to the array line; and h_n is the height of an element. The agreement seems to be fairly good with respect to -3db beamwidth and front to back ratio. The calculated beamwidth is broader than the measured one. This characteristic is even more evident in Figure 13, which compares measured and calculated beamwidths for Case D. (This again is a typical pattern.) A broader calculated H-plane beamwidth is in agreement with the results of Carrel,²² which is not surprising, since the \bar{Z}_a matrix formulation is the same as Carrel's. Both Carrel and Cheong²³ cite the sinusoidal approximation as the reason for errors in the radiation patterns.

Figure 14 shows the measured and calculated input impedance for Case A₃. The average impedance is

slightly lower for the computed data and the VSWR is slightly higher. Figure 15 compares measured and calculated impedances for Case C₃. The agreement here is seen to be quite good both with respect to average impedance and VSWR. The calculated data here is obtained using a \bar{Y}_f matrix formulation based on the measured locus in Figure 11. Figure 15A compares the computed data in Figure 15 with computed data obtained from a \bar{Y}_f matrix formulation based on (44) and (45). Cases C₃ and D were both tested in this way, and the agreement between both methods of \bar{Y}_f matrix formulation was quite good.

Figure 16 summarizes all the Case A and Case B data. In general, the computed average impedance is lower and the computed VSWR is higher than the corresponding measured values.

Figure 17 compares the measured and computed impedances of Case D. Again, we see that the computed average impedance is lower and the computed VSWR is higher than the corresponding measured quantities. An isolated shunt-fed monopole having the same feed capacitor and support arrangement as the monopoles in Case D had to be measured to obtain the resonant impedance for this case, since the effective diameters of these monopoles are not constant over their entire length, and

Figure 6 could not be used. It is interesting to note that the resonant impedance obtained for an H/h of 0.1 was 11.5 ohms which is the same as for a uniform cross-section monopole with $H/h = .1$ and $h/a=30$ (h/a for Case D is 60). All experiments attempting to match this antenna, to a reasonable VSWR with respect to 50 ohms, without the outer vertical capacitor supports were unsuccessful. The reason remains unexplained.

It was the antenna of Case D which provided the experimental evidence leading to the technique, using a $\tau' > \tau$ for determining capacitor lengths, for optimizing the impedance match. A description of the experimental process of impedance optimization may be of interest. After selecting the log-periodic parameters of $\tau=0.82$ and $\sigma=0.15$ from the dipole data of Carrel and adding the outer capacitor supports, the following additional initial parameters were selected; $y_n = s_{n-1}$, $H_n = 0.1 h_n$, and $Z_{c_0} = 51$ ohms. This yielded a maximum VSWR of 3.2 with respect to 63 ohms. Raising H_n to $0.12 h_n$ improved the average VSWR slightly but did not change the average impedance. With $Z_{c_0} = 34$ ohms, $y_n = s_{n-1}$ and $H_n = 0.12 h_n$, the nominal impedance dropped to 43 ohms, but the VSWR rose to 8; H_n was decreased to $0.1 h_n$, and the average VSWR dropped, but a VSWR of 8 persisted at the lower

frequencies. y_n was now decreased so that $y_n = (s_{n-1})/2$. The average VSWR remained about the same, but the higher VSWR values were now at the higher frequencies. It appeared as if the capacitor lengths should be changed by some other ratio than the log-periodic constant τ . With the front capacitor assumed to be $y_1 = s_0 = \tau s_1$, and the rear capacitor assumed to be $y_{11} = s_{10}/2$, a constant $\tau' = (y_1/y_{11})^{1/10} = (2\tau s_1/s_{10})^{1/10} = 2^{1/10} \tau$ was calculated. $2^{1/10} \tau = 0.8785 \approx 0.88$. The use of this ratio together with a slight increase in all capacitor lengths resulted in a VSWR of less than 2 with respect to an average impedance of about 44 ohms. See Figure 17.

At this time Fred R. Ore sent me a copy of his report on the Wire-Outline monopole array with which he obtained "optimum" impedance match by step-tapering his feed rod to obtain less proportionate capacity at the rear of the antenna. A model was built, the antenna in Figure 1, to see if the method used on the antenna in Figure 2 would work with Ore's Wire-Outline monopole array. The successful result of this experiment is Case C₃, which suggests that the length taper and the feed-rod diameter step-taper used by Ore are approximately equivalent, although the length taper is more easily implemented.

Why does this length taper improve the impedance match? The answer is connected with the rate of taper of Z_{O_n} values calculated or measured when operating the entire structure in the transmission region. A comparison of the values calculated for Cases A₃ and C₃ is enlightening. For A₃, an unsuccessful design, $Z_{O_1}=71.5$ and $Z_{O_5}=85.8$, while for C₃, a successful design, $Z_{O_1}=73.6$ and $Z_{O_5}=103.0$. The ratio of Z_{O_5} to Z_{O_1} is 1.2 in the first case and 1.4 in the second case. Of even greater interest are the cutoff frequencies of the equivalent Π or T networks for both cases. For Case A₃ section 4 has a cutoff frequency of 780 MHz, and Case C₃ has a cutoff frequency of 843 MHz. It so happens that section 4 is in the active region of the antenna at 720 MHz, which suggests that Case A₃ may be very close to a stop-band situation, especially when one considers that the loading of the line within the active region may cause an even lower cutoff frequency due to the lower V_p . A recent publication by Ingerson and Mayes²⁴ tends to support this supposition.

A possible explanation for the consistently lower characteristic impedances obtained in Cases A and B is suggested by Figure 18. The matching networks for these cases and for Case C₃ were calculated for a transformation from 33.5 ohms to whatever resistance value

a given feedpoint height H required. The calculated self-impedance is 27.5 ohms, which is about 20 percent less than the 33.5 ohm value obtained from King's²⁵ second order approximation curve, the dashed locus in Figure 18.

CONCLUSIONS

A method of analysis, related to the Log-Periodic Dipole analysis of Carrel,⁵ for the analysis of shunt-fed log-periodic monopole arrays has been presented. Calculated data has been compared with experimental data and a reasonable degree of correlation obtained. The method of analysis suggests an explanation for the success of experimental impedance optimization. The key to the success of the analysis is in the calculation of the feeder admittance matrix which it is shown may be calculated entirely from physical dimensions of the antenna.

BIBLIOGRAPHY

1. A. F. Wickersham, Jr., "Recent Developments in Very Broadband End-Fire Arrays," *Proceedings of the I.R.E.*, April 1960, pp. 794-795.
2. A. F. Wickersham, Jr. *et al.*, "Further Developments in Tapered Ladder Antennas," *Proceedings of the I.R.E.*, January 1961, p. 378.
3. F. R. Ore, "A Coaxial Fed Unidirectional Log-Periodic Monopole Array," *Collins Radio Company*, Cedar Rapids, Iowa, August 1961.
4. D. E. Isbell, "Log Periodic Dipole Arrays," *Antenna Laboratory Technical Report No. 39*, University of Illinois, Urbana, Illinois, June 1959.
5. R. L. Carrel, "Analysis of the Log-Periodic Dipole Array," *Antenna Laboratory Technical Report No. 52*, University of Illinois, Urbana, Illinois, October 1961.
6. E. Hudock and P. E. Mayes, "Near Field Investigation of Uniformly Periodic Monopole Arrays," *Trans. IEEE*, Vol. AP-13, No. 6, November 1965, pp. 840-855.
7. Ore, *op. cit.*, p. 10.

8. Carrel, *op. cit.*, pp. 21-38.
9. *Ibid.*, pp. 26-33.
10. H. E. King, "Mutual Impedance of Unequal Length Antennas in Echelon," *IRE Transactions*, Vol. AP-5, No. 3, July 1957, pp. 306-313.
11. Weng-Meng Cheong, "Arrays of Unequal and Unequally Spaced Dipoles, with Application to the Log-Periodic Antenna," *Scientific Report No. 14 (series 3) Contract AFL9(628)-2406*, Craft Laboratory, Harvard University, Cambridge, Mass., December 1966.
12. Weng-Meng Cheong and Ronold W. P. King, "Arrays of Unequal and Unequally Spaced Dipoles," *Radio Science*, Vol. 2, No. 11, November 1967, pp. 1303-1314.
13. Weng-Meng Cheong and Ronold W. P. King, "Log-Periodic Dipole Antenna," *Radio Science*, Vol. 2, No. 11, November 1967, pp. 1315-1325.
14. Carrel, *op. cit.*, pp. 31-33.
15. P. S. Carter, "Circuit Relations in Radiating Systems and Application to Antenna Problems," *Proceedings of the I.R.E.*, Vol. 20, June 1932, pp. 1004-1041.
16. Carrel, *op. cit.*, p. 27.

17. J. F. Morrison and P. H. Smith, "The Shunt Excited Antenna," *Proceedings of the I.R.E.*, Vol. 25, June 1937, pp. 673-696.
18. *Ibid.*
19. Carrel, *op. cit.*, pp. 39-77.
20. Ore, *op. cit.*, Figure 7.
21. S. Uda and Y. Mushiake, "Yagi-Uda Antennas," Maruzen Co., Ltd., Tokyo, 1954, p. 19.
22. Carrel, *op. cit.*, p. 102.
23. Weng-Meng Cheong, *op. cit.*, pp. 10-15a - 10-15b.
24. P. G. Ingerson and P. E. Mayes, "Log-Periodic Antennas with Modulated Impedance Feeders," *Trans, IEEE*, Vol. AP-16, No. 6, November 1968, pp. 633-642.
25. R. W. P. King, "The Theory of Linear Antennas," University of Harvard Press, Cambridge, Mass., 1956, p. 169.

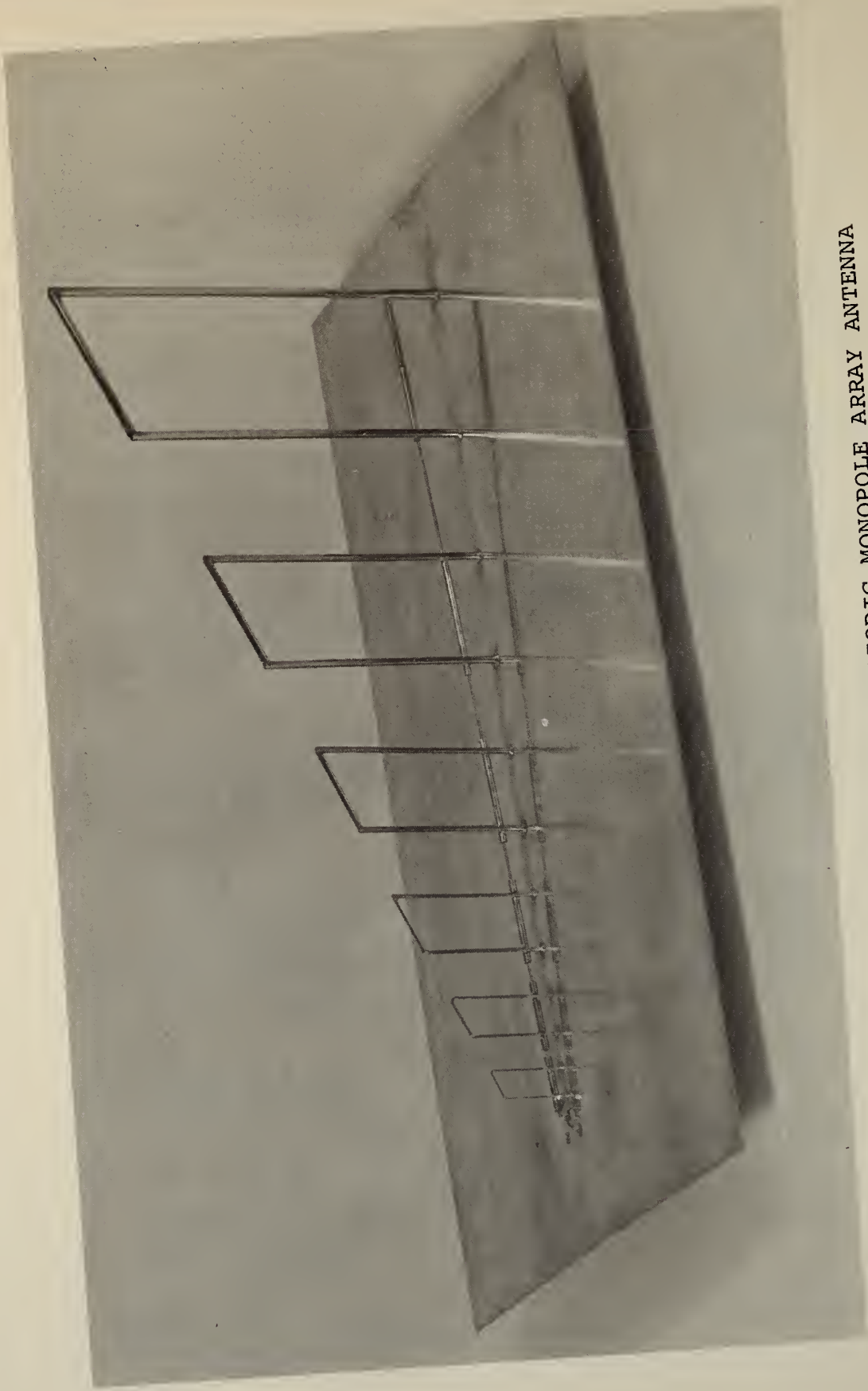


Figure 1. A SHUNT-FED LOG-PERIODIC MONOPOLE ARRAY ANTENNA
OF THE WIRE-OUTLINE TYPE



Figure 2. A SHUNT-FED LOG-PERIODIC MONOPOLE ARRAY ANTENNA
WITH CYLINDRICAL MONOPOLES

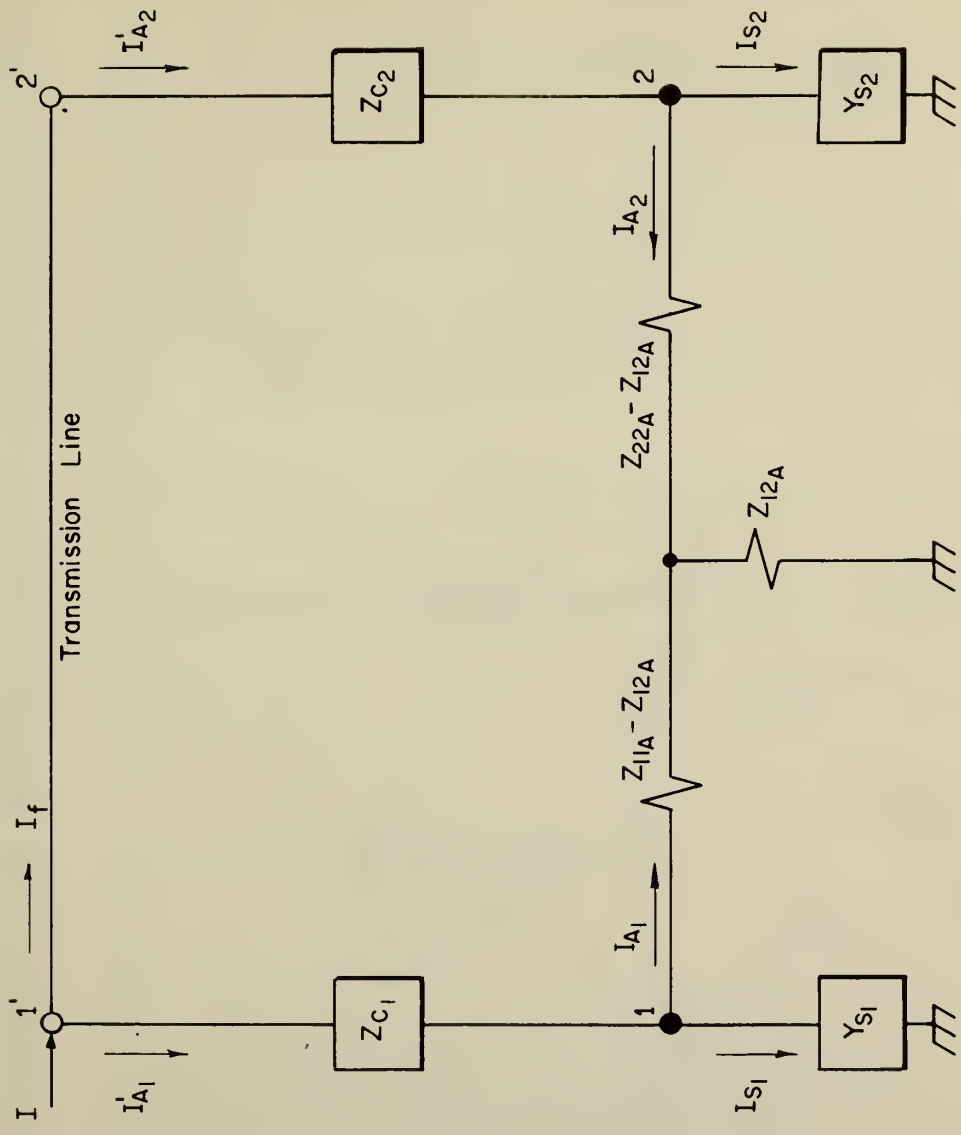


Figure 4. DIAGRAM OF A TWO-ELEMENT SHUNT-FED ARRAY ILLUSTRATING EQUIVALENT CIRCUIT ELEMENTS AND NODE CURRENT RELATIONS.

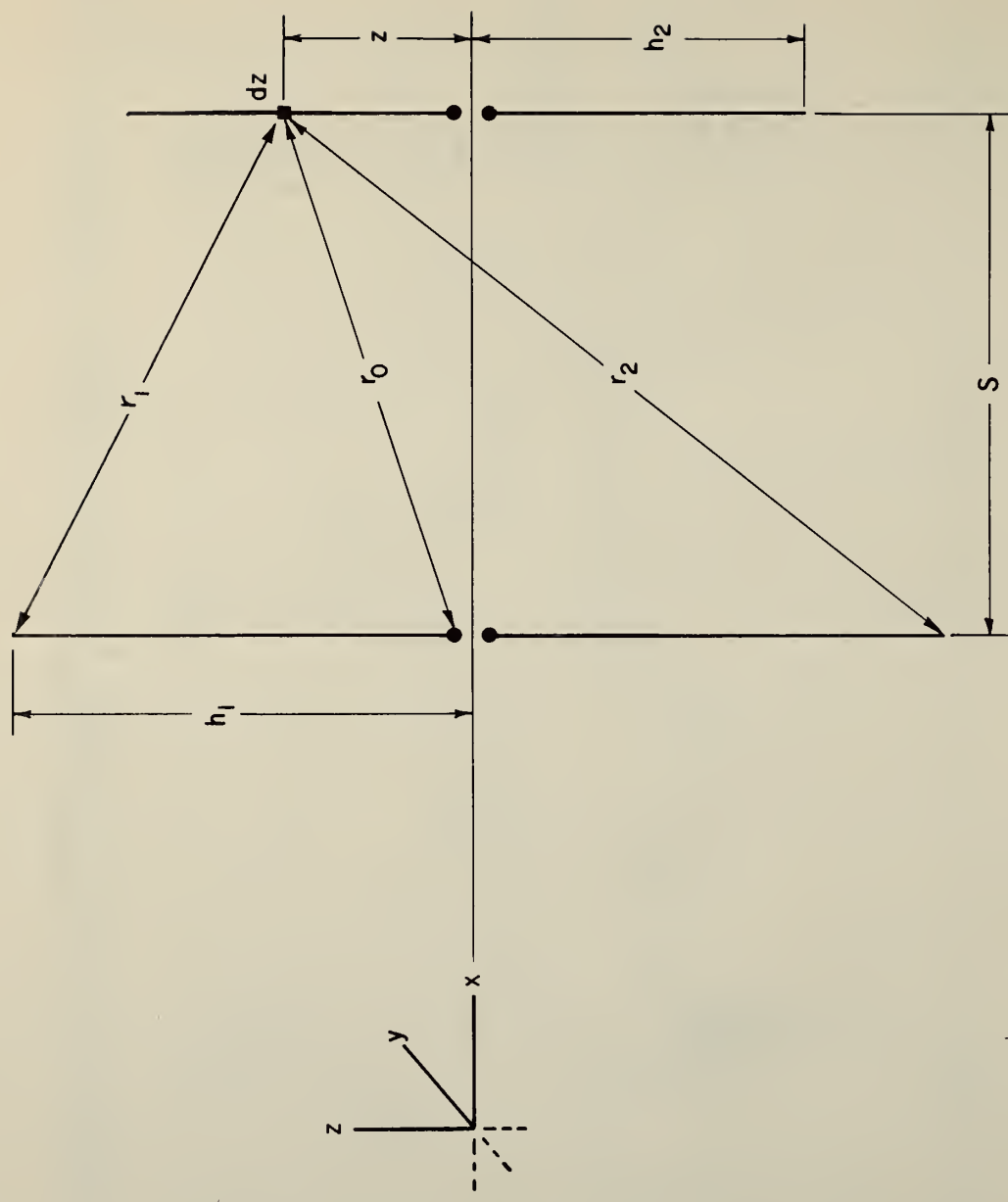


Figure 5. GEOMETRY AND NOTATION USED IN MUTUAL IMPEDANCE CALCULATIONS

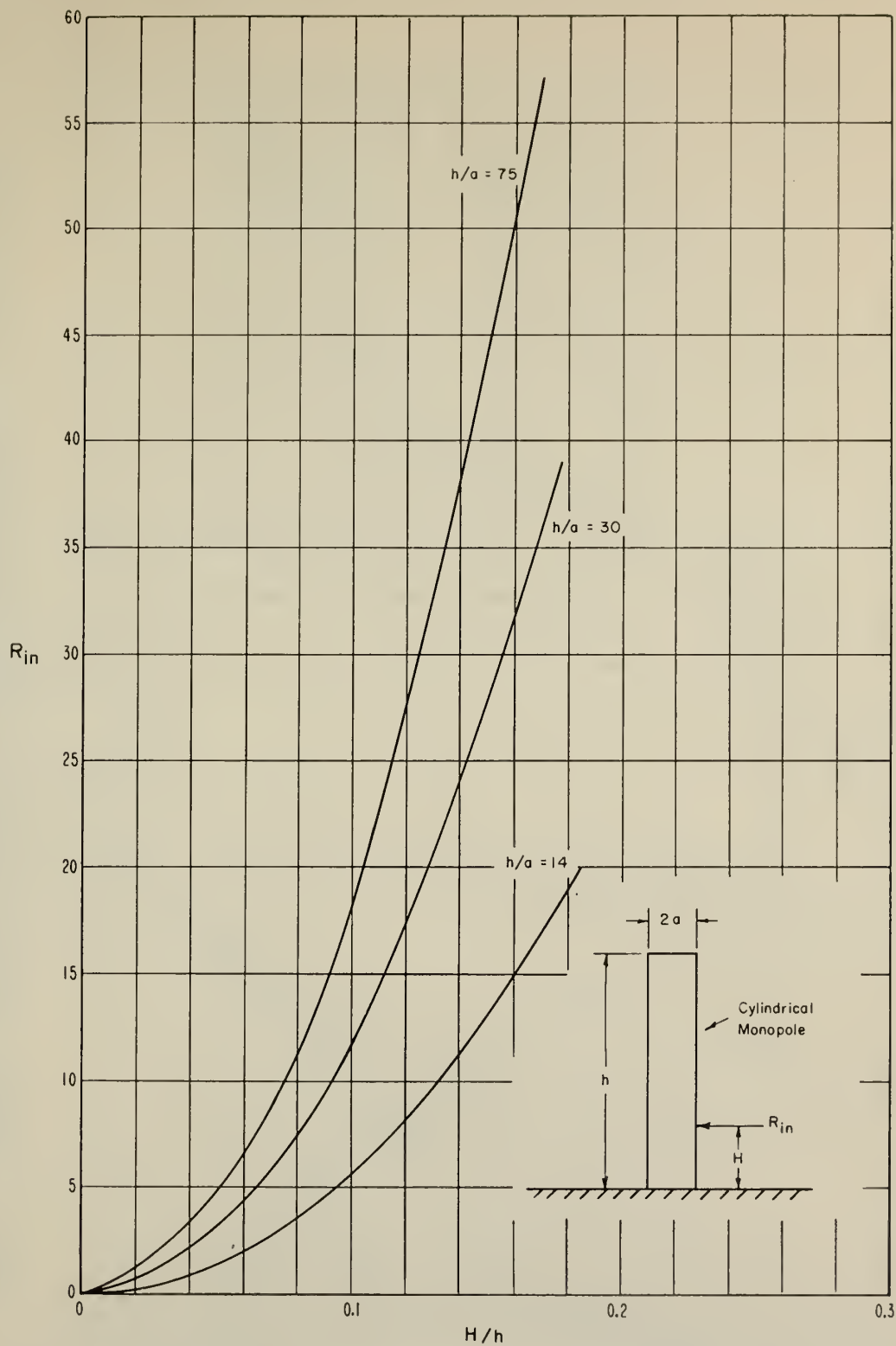


Figure 6. RESONANT IMPEDANCE OF A SHUNT-FED MONOPOLE AS A FUNCTION OF FEEDPOINT HEIGHT WITH HEIGHT TO RADIUS RATIO AS PARAMETER.

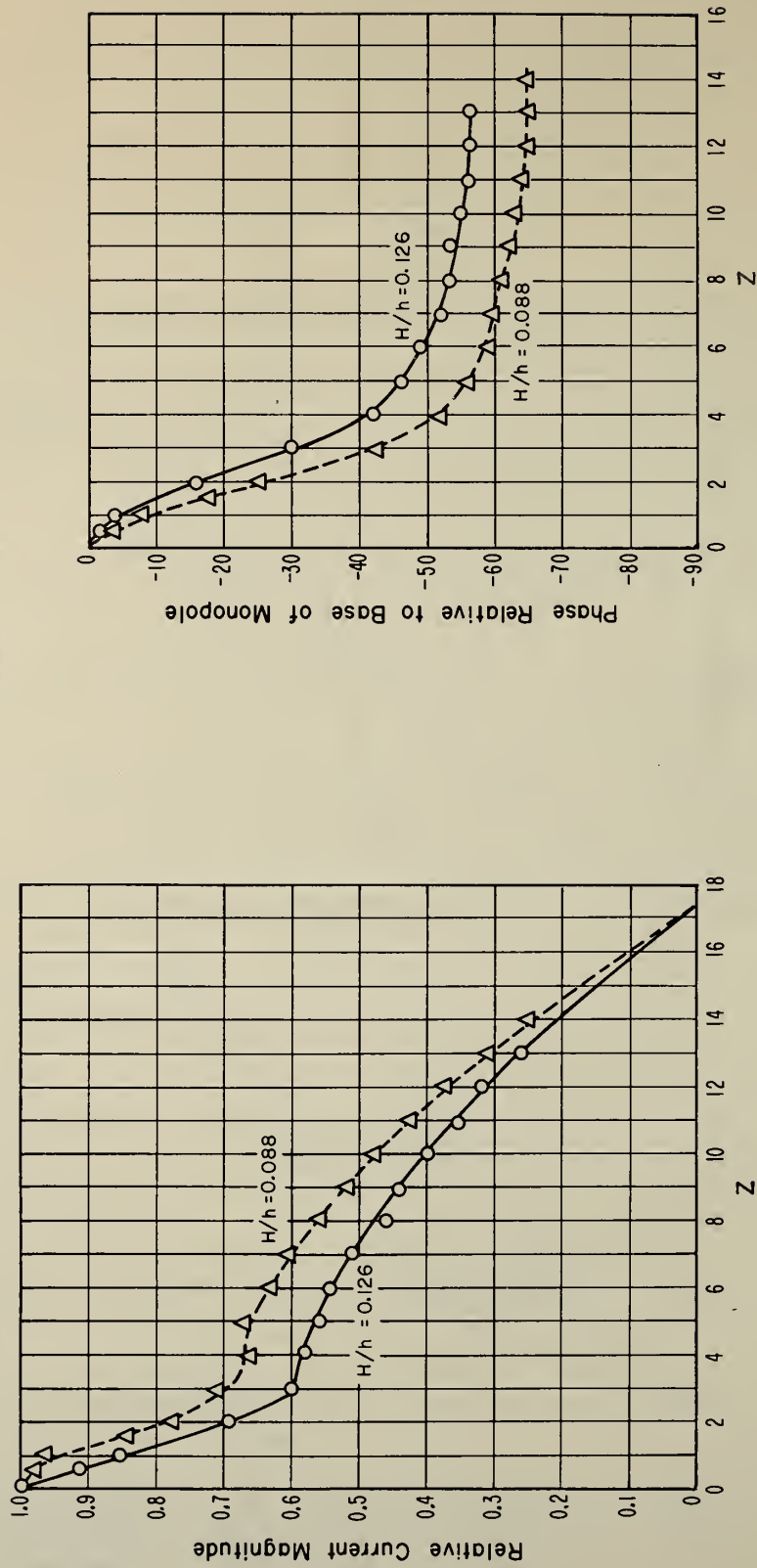
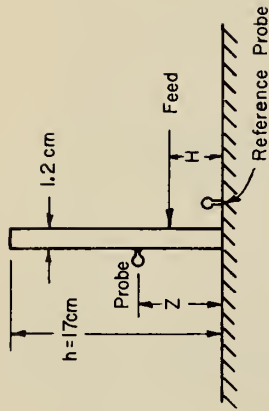


Figure 7. CURRENT DISTRIBUTION ON A SHUNT-FED MONOPOLE VS PROBE HEIGHT WITH FEED-POINT HEIGHT AS A PARAMETER. $f = 400\text{ MHz}$, $h/a = 29$

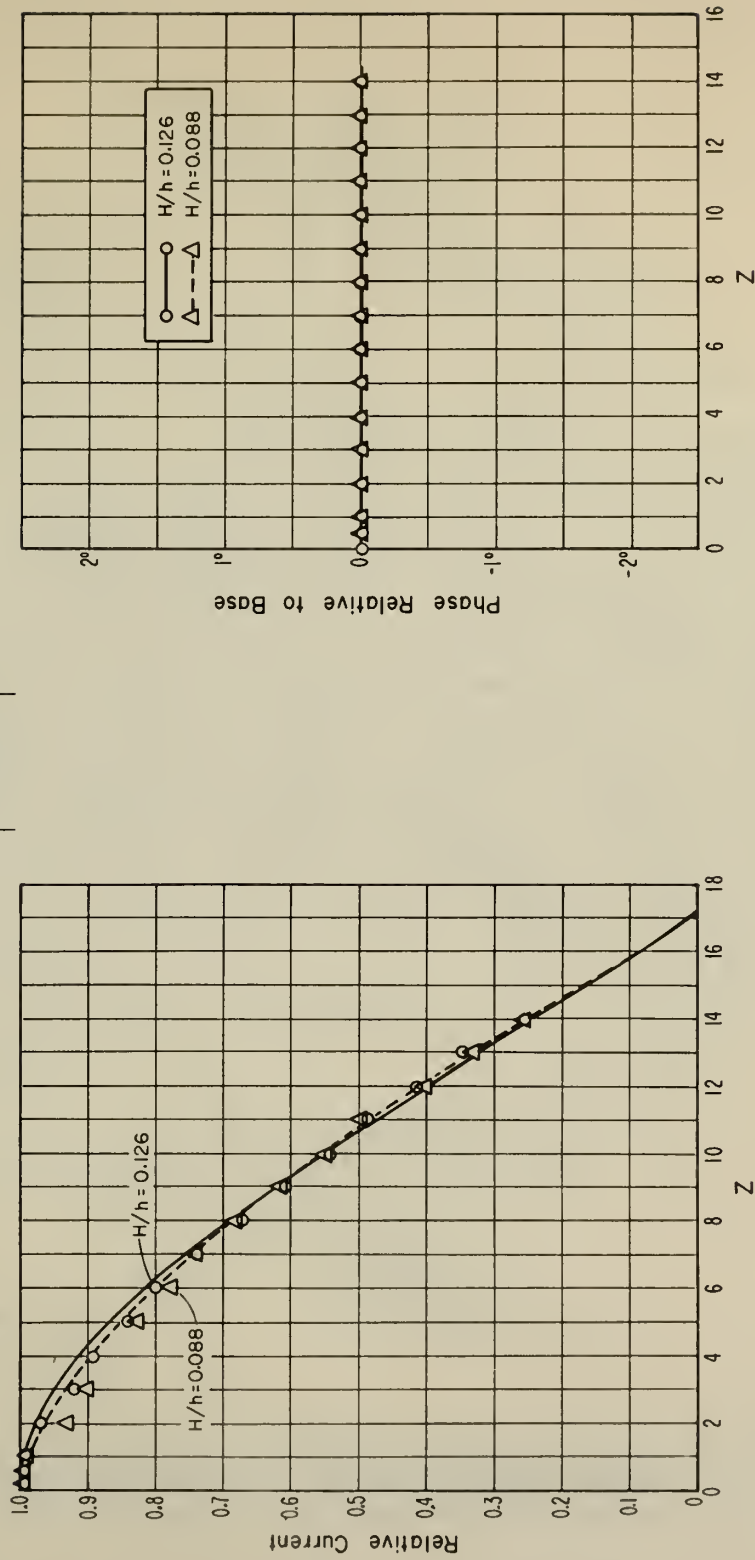
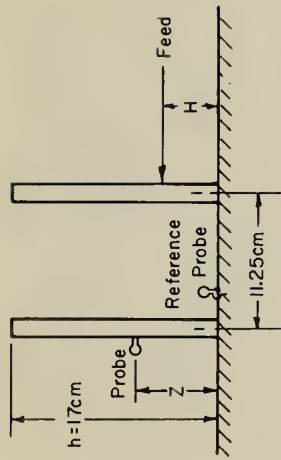
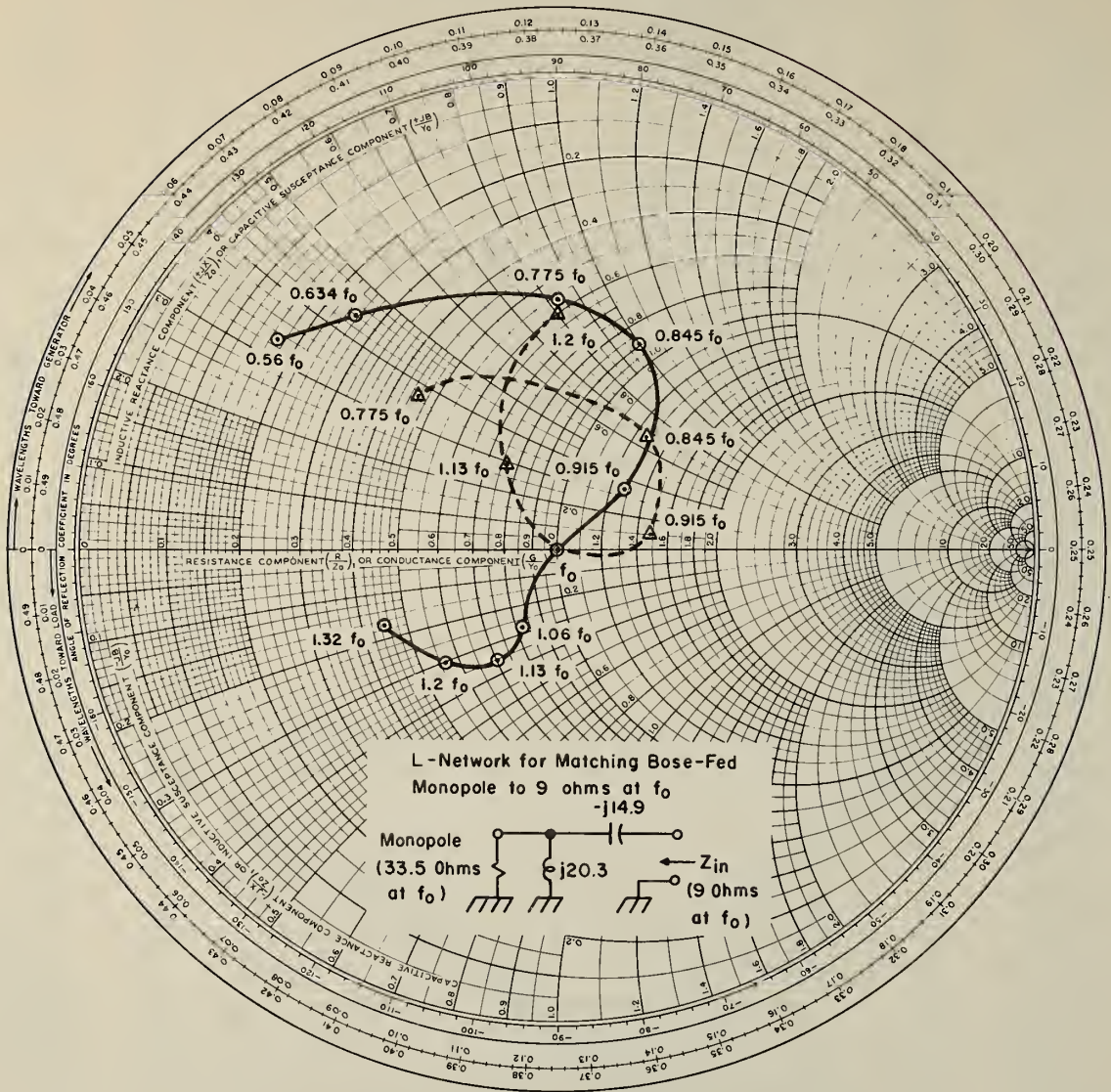


Figure 8. CURRENT DISTRIBUTION ON A GROUNDED MONOPOLE VS PROBE HEIGHT.
 CURRENT INDUCED BY ADJACENT SHUNT-FED MONOPOLE OF EQUAL HEIGHT.
 FEED-POINT HEIGHT IS PARAMETER. $f = 400\text{MHz}$, $h/a = 29$

IMPEDANCE OR ADMITTANCE COORDINATES



- $h/\lambda = 14$ for both monopoles
- $h/\lambda = 0.126$ for shunt-fed monopole
- \circ Shunt-fed monopole.
- \triangle Base fed monopole with matching network.
(Network shown above)

Figure 9. INPUT IMPEDANCE VS. FREQUENCY OF A SHUNT-FED MONOPOLE AND A BASE FED MONOPOLE WITH A MATCHING NETWORK. VALUES ARE NORMALIZED TO 9 OHMS.

IMPEDANCE OR ADMITTANCE COORDINATES

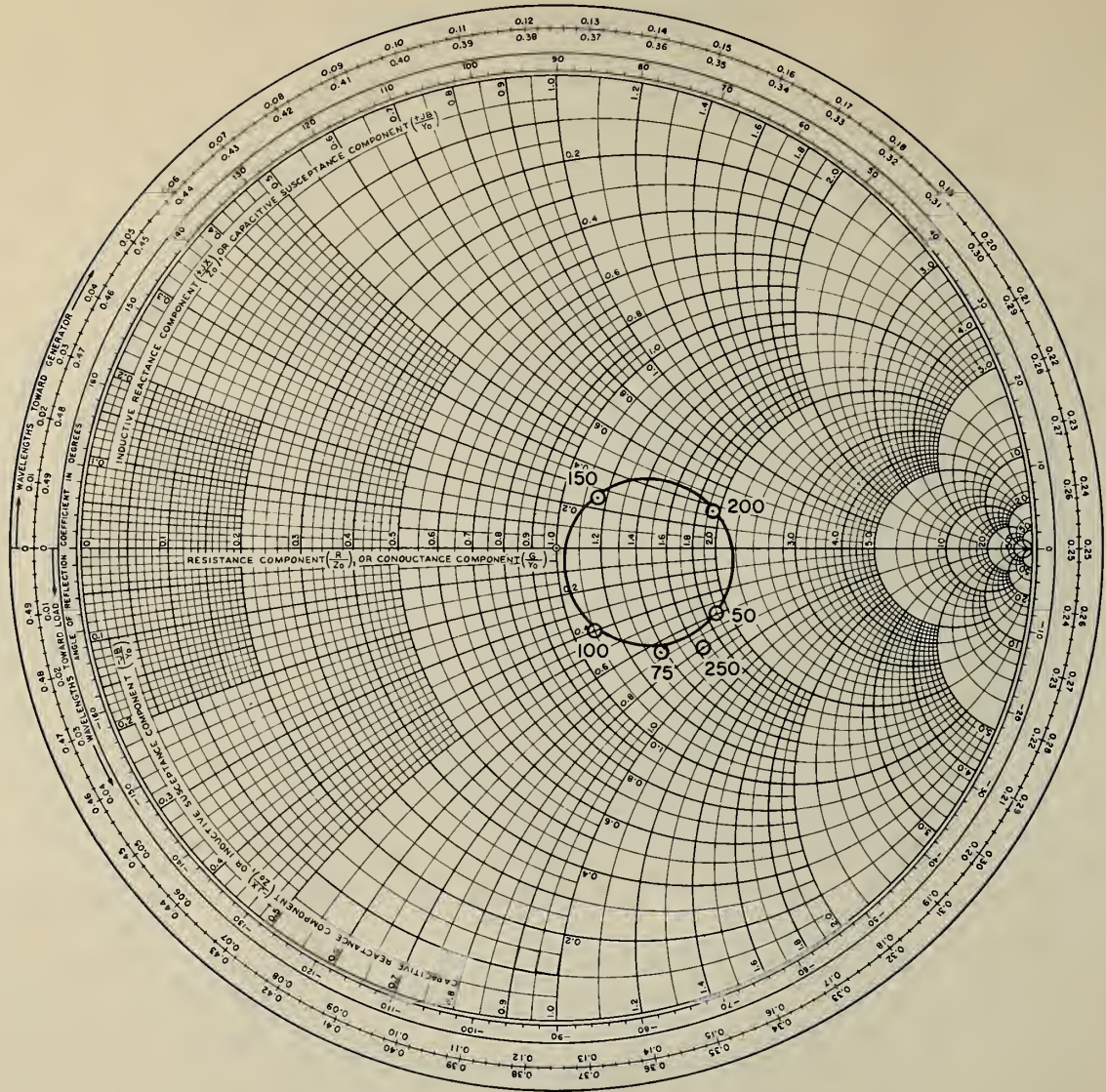


Figure 11. LOCUS FOR Z_0 AND V_p DETERMINATION FOR CASE C_3 . ANTENNA FEEDER IS TERMINATED IN A 150 Ω RESISTOR.

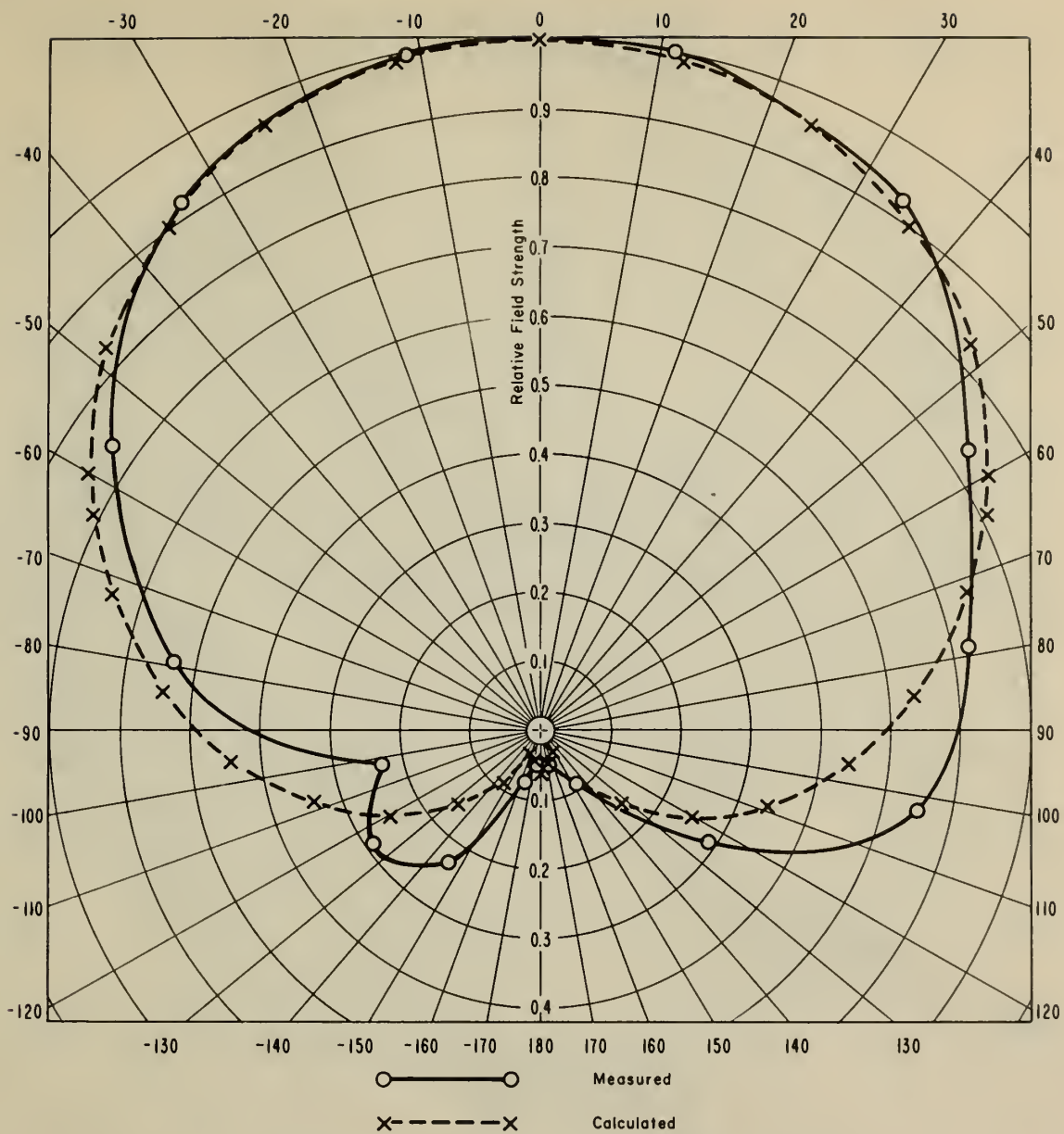


Figure 12. MEASURED AND CALCULATED RADIATION PATTERNS FOR CASE C_3 IN AZIMUTH PLANE. (E_θ vs. ϕ for $\theta=90^\circ$) ARRAY VERTEX AT $\phi = 0^\circ$ FREQUENCY IS 720 MHz

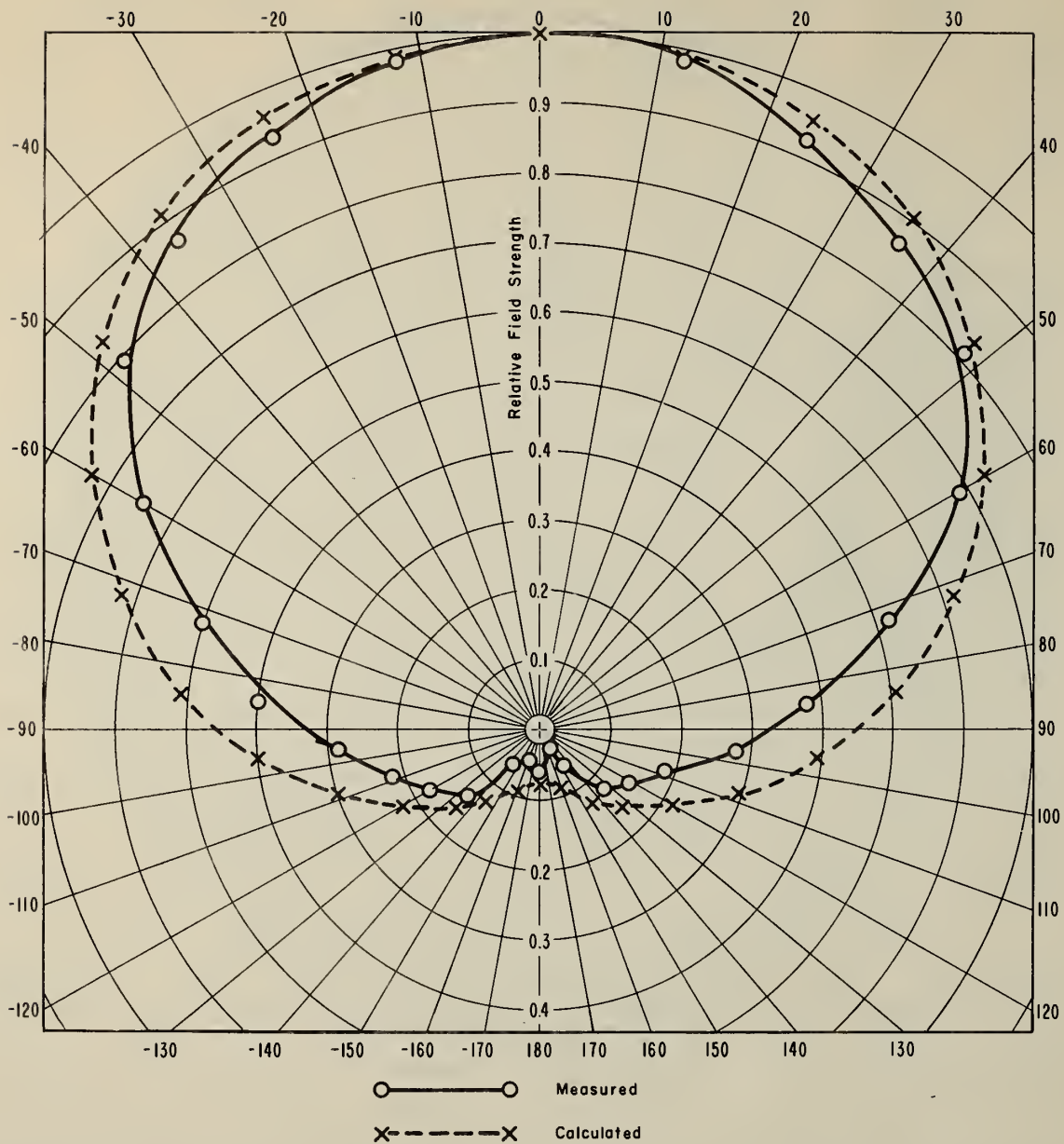
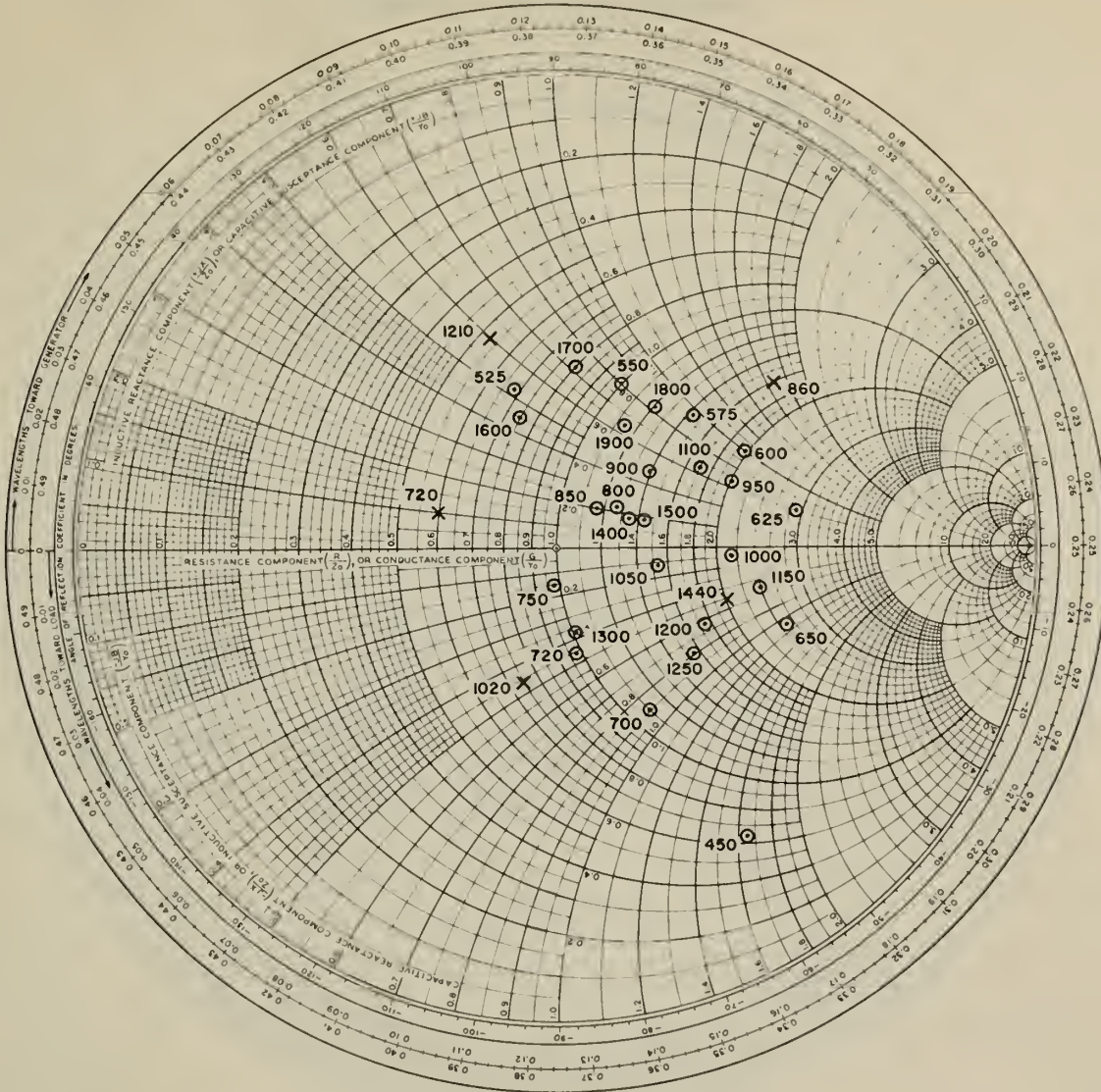


Figure 13. MEASURED AND CALCULATED RADIATION PATTERNS FOR CASE D IN AZIMUTH PLANE. (E_θ vs ϕ for $\theta=90^\circ$) ARRAY VERTEX AT $\phi=0^\circ$ FREQUENCY IS 943 MHz

IMPEDANCE OR ADMITTANCE COORDINATES

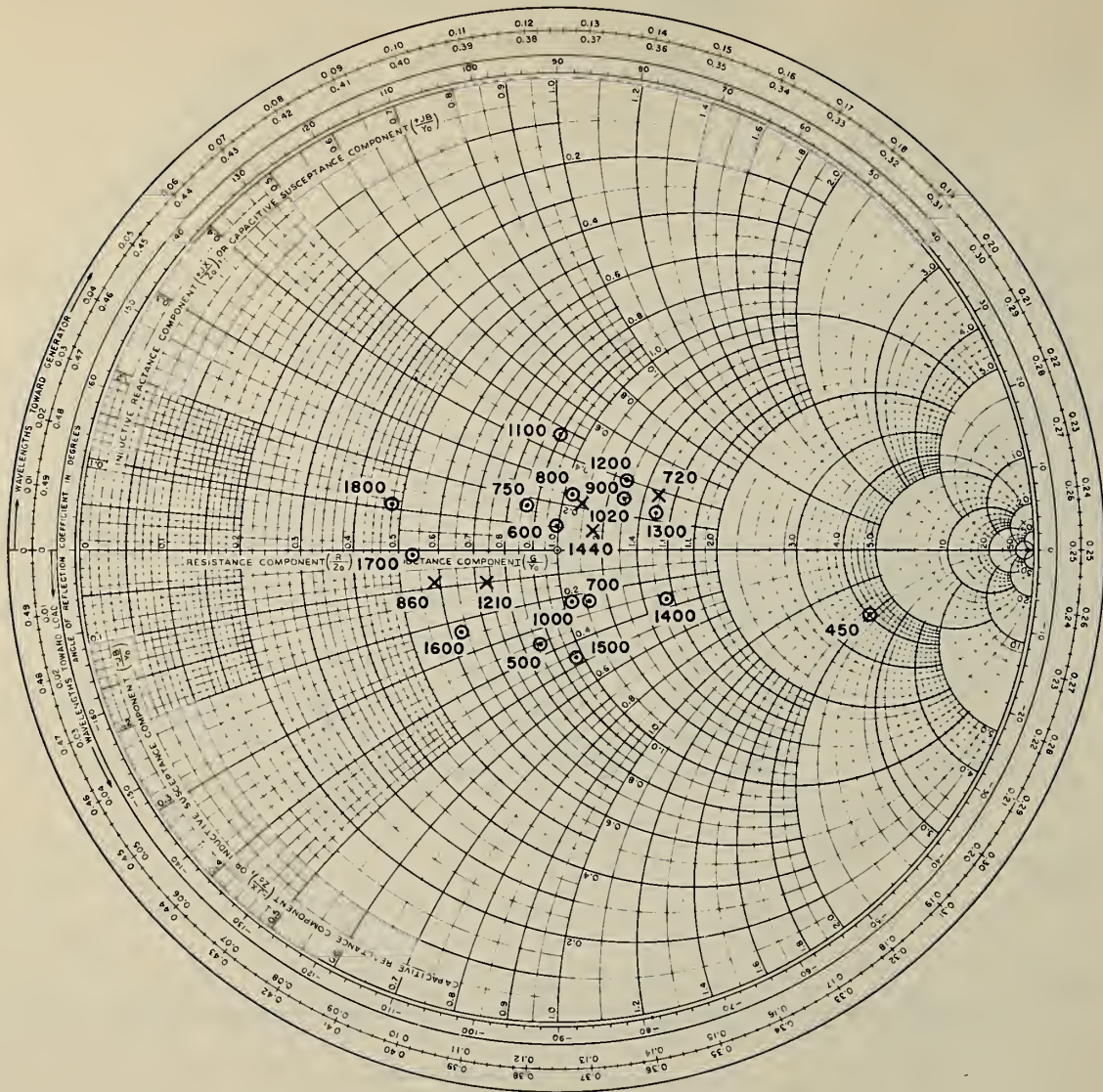


$\tau = \tau$
 $Z_{co} = 52 \text{ Ohms}$
 $H_n/h_n = 0.126$

⊙ Experimental Points
 X Calculated Points

Figure 14. INPUT IMPEDANCE OF WIRE-OUTLINE MONOPOLE ARRAY VS. FREQUENCY FOR CASE A₃. VALUES NORMALIZED TO 50 OHMS.

IMPEDANCE OR ADMITTANCE COORDINATES

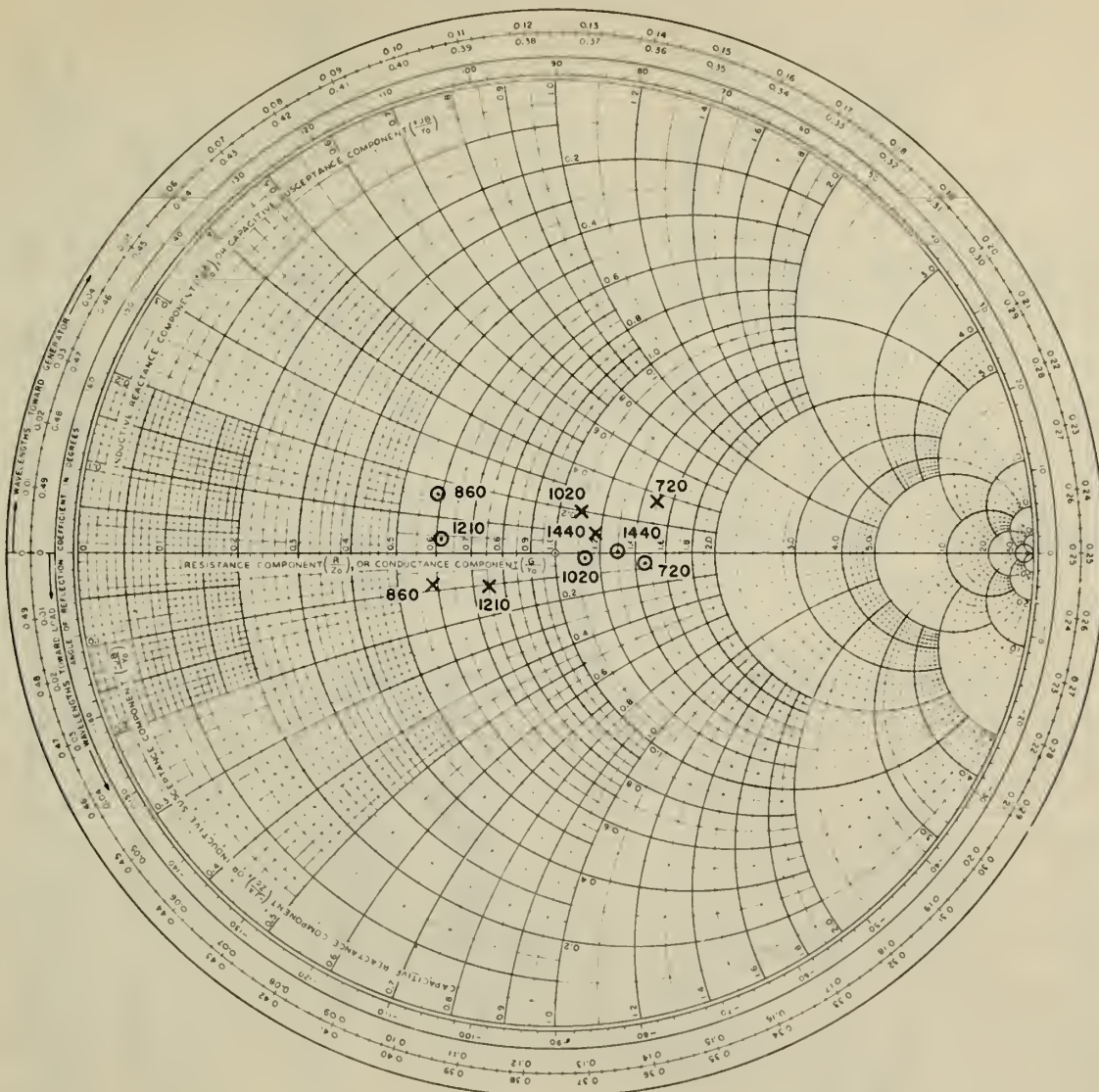


$\tau' = 0.8$
 $Z_{c0} = 42.8$ Ohms
 $H_n/h_n = 0.126$

○ Experimental Points
 × Calculated Points

Figure 15. INPUT IMPEDANCE OF WIRE-OUTLINE MONOPOLE ARRAY VS. FREQUENCY FOR "OPTIMIZED" FEED (Case C₃) VALUES NORMALIZED TO 50 OHMS.

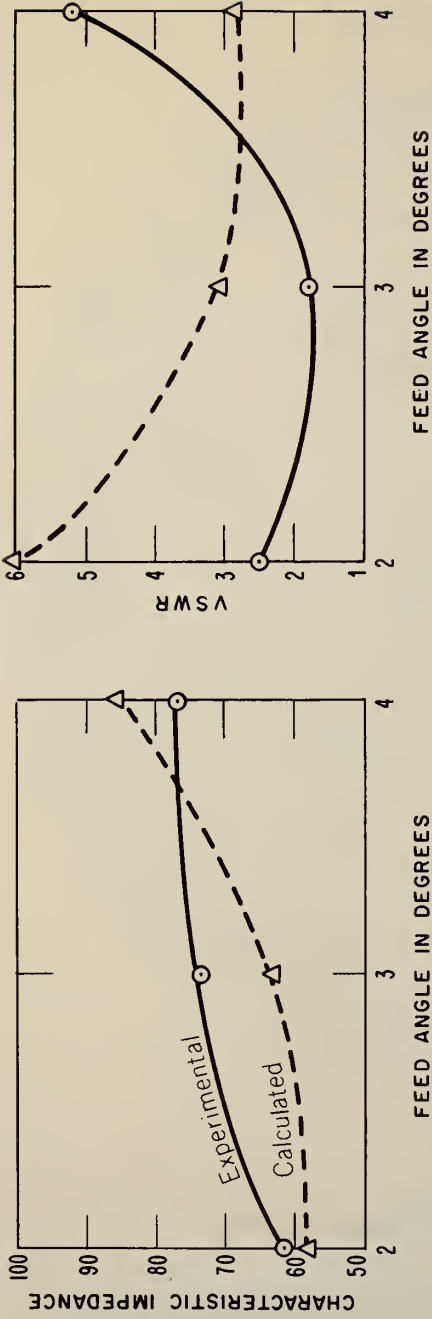
IMPEDANCE OR ADMITTANCE COORDINATES



- X Calculated data with V_p and Z_{0n} obtained by experiment.
- O Calculated data with V_p and Z_{0n} calculated.

Figure 15A A COMPARISON OF CALCULATED IMPEDANCES FOR CASE C₃
 (V_p and Z_0 data for Y_f matrix calculations obtained in different ways)

CASE A



CASE B

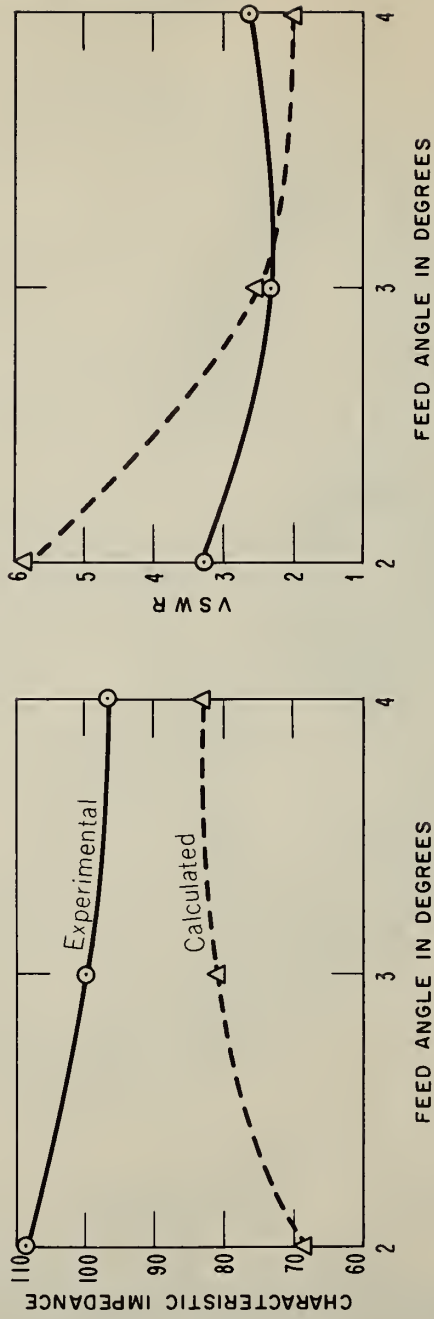
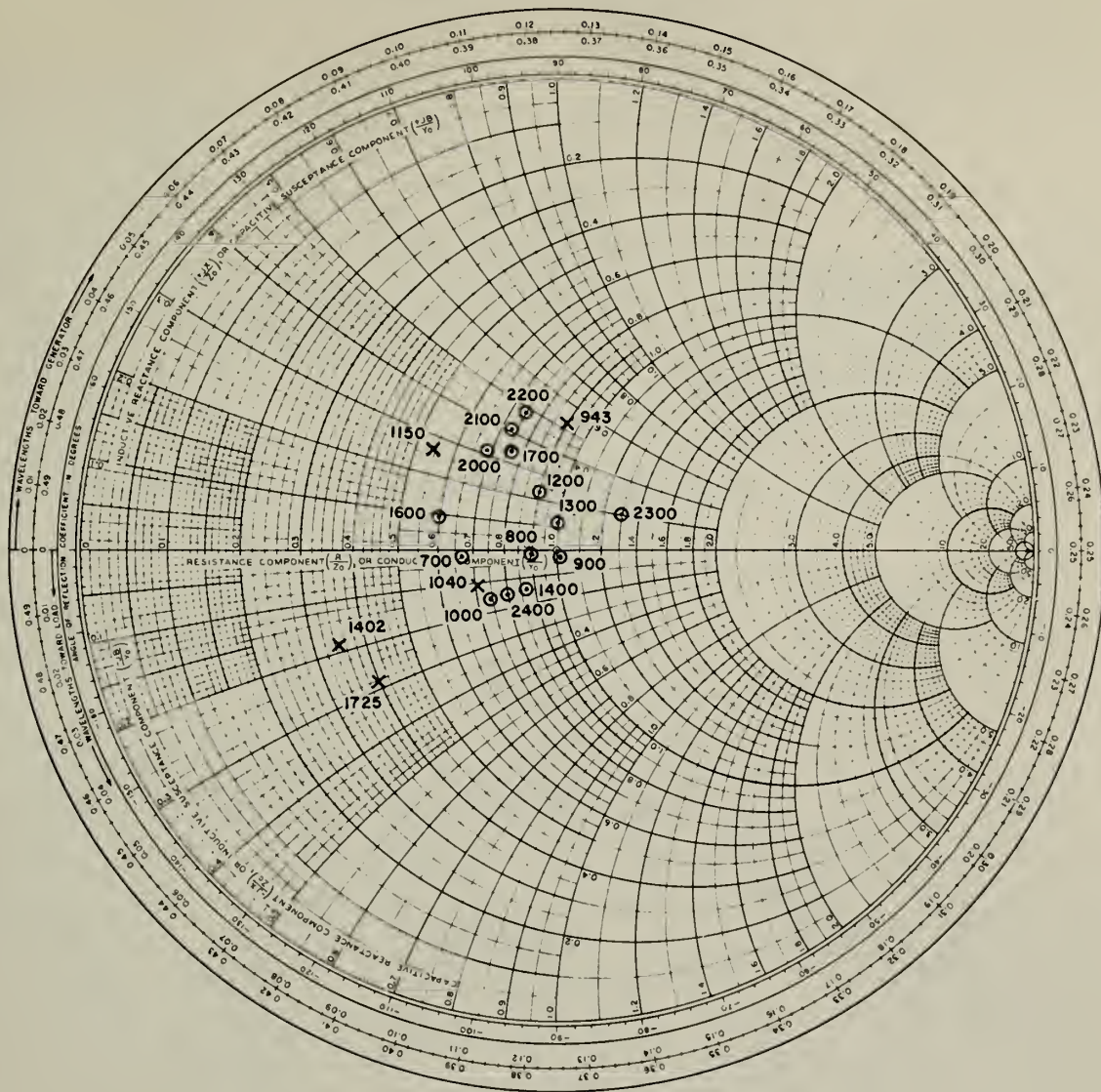


Figure 16. AVERAGE CHARACTERISTIC IMPEDANCE AND VSWR OF CASES A AND B. A COMPARISON OF MEASURED AND CALCULATED DATA. (Data is for frequencies from 720-1440 MHz)

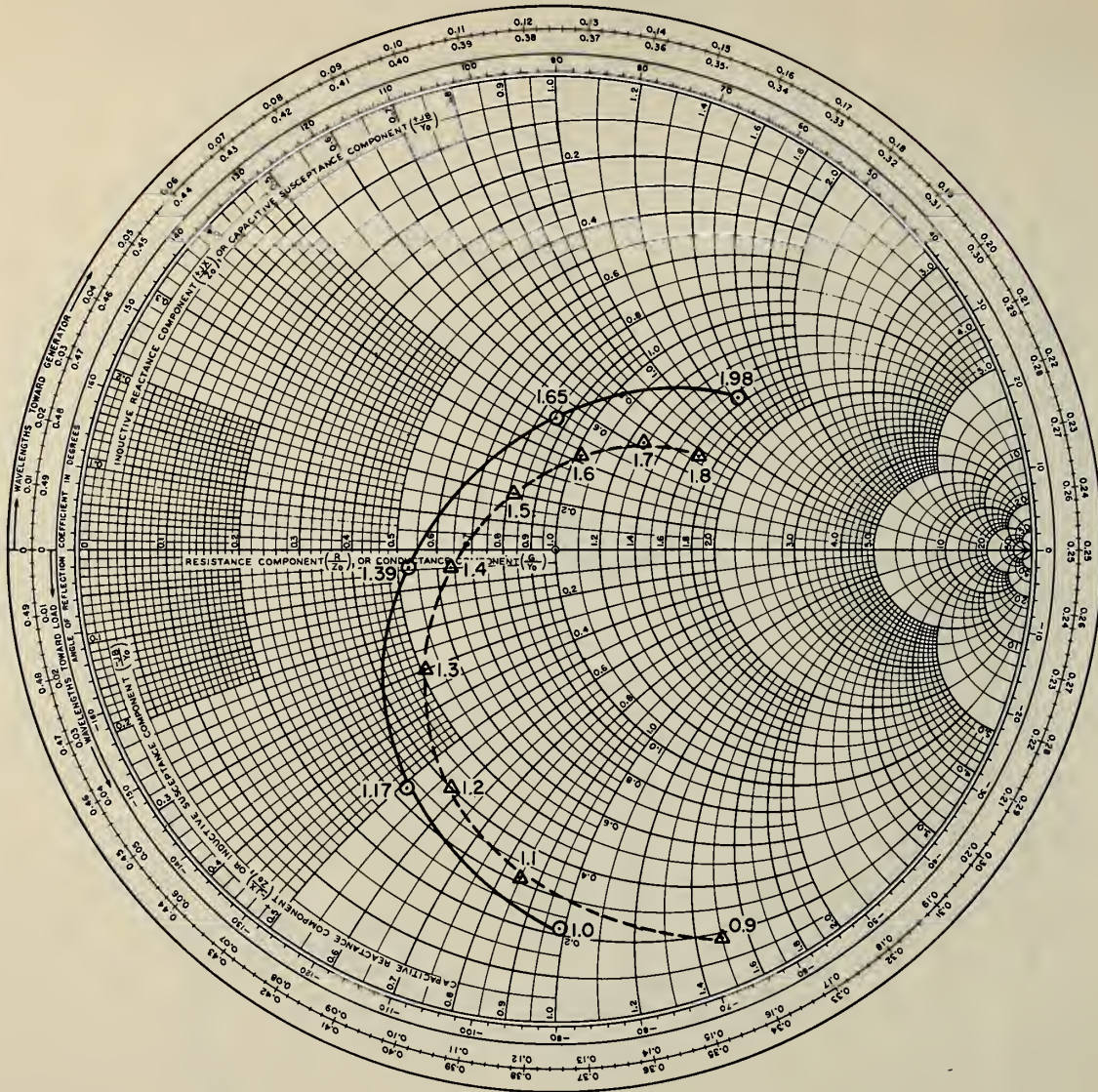
IMPEDANCE OR ADMITTANCE COORDINATES



$\tau^1 = 0.88$ \odot Experimental Points
 $Z = 33.5$ Ohms \times Calculated Points
 $h_n/h_\eta = 0.1$

Figure 17. INPUT IMPEDANCE OF CYLINDRICAL MONOPOLE ARRAY VS. FREQUENCY FOR CASE D. VALUES NORMALIZED TO 50 OHMS.

IMPEDANCE OR ADMITTANCE COORDINATES



○——○ Computed Herein for $h/a=14$
 △-----△ King's 2nd Order Approx. for $h/a=16.5$

Figure 18. COMPUTED SELF IMPEDANCES FOR MONOPOLES AS A FUNCTION OF ELECTRICAL LENGTH, IN RADIAN, FOR CONSTANT h/a . (IMPEDANCES NORMALIZED TO 50Ω)



PENN STATE UNIVERSITY LIBRARIES



A000072011867